Seismic Design and Performance of Buckling Restrained Braced Frames with Eccentric Brace Configurations Part 1: Design Procedure and Case Studies

CHAO-HSIEN LI, PAUL W. RICHARDS, BRANDT W. SAXEY, and HEIDI L. RICHARDS

ABSTRACT

Buckling-restrained braced frames (BRBFs) are a widely used lateral system comprised of beams, columns, and diagonal buckling restrained braces (BRBs). The BRBs within these frames are typically oriented concentrically. Current U.S. design provisions limit the eccentricities in BRBFs to less than the beam depth, which results in less architectural flexibility as compared to eccentrically braced frames (EBFs). The purpose of the present study is to investigate the design and performance of BRBFs with larger beam eccentricities. BRBFs were designed with beam eccentricities ranging from 0 (control case) to 2 times the beam depth in the chevron (inverted-V) and single-diagonal configurations. In each case, the beams were designed to remain elastic under the maximum forces that could be delivered by the braces, including the effects of the brace eccentricity on the beam. Nonlinear response history analysis and pushover analysis were used to quantify the performance of the various frames under design earthquake shaking and to investigate the relationship between BRBF beam eccentricity and seismic performance for the cases considered. The results of this study are presented in a two-part paper. This paper, constituting Part 1, describes the design procedures for BRBFs with eccentricity in chevron and single-diagonal configurations. Analysis methods for determining force demands in braces, beams, and columns are presented. The analysis methods are illustrated through the design of nine case study buildings. The designs show the impact that eccentricities have on member sizing and overall frame weight. For chevron BRBFs, eccentricities of 1 to 2 times the beam depth resulted in overall frame weight increase of 1.07 to 1.32 times, due to heavier beams. For single-diagonal BRBFs, eccentricities of 2 times the beam depth resulted in a slight reduction of overall weight, due to moment frame action associated with the eccentric beam stub. The accompanying paper, Part 2 (Li et al., 2026), presents the nonlinear analysis studies, including response history analyses and pushover analysis, for evaluating the seismic performance of these nine case study designs.

Keywords: buckling restrained braced frames, eccentric bracing, eccentric braced frames.

INTRODUCTION

In the late 1970s and through the 1980s, there was a focused research effort to develop a ductile braced frame for U.S. practice. Eccentrically braced frames (EBFs) were viewed as a way to combine the desirable stiffness of braced frames, with the desirable ductility and architectural flexibility of moment frames. Experimental and analytical studies at Berkeley investigated isolated EBF yielding links, subassemblies, and systems (Engelhardt and Popov, 1992; Hjelmstad and Popov, 1983; Kasai and Popov, 1986; Malley and Popov, 1984; Roeder and Popov, 1978). Provisions for EBF design were included in the original AISC *Seismic Provisions for Structural Steel Buildings* (1990) and were updated in subsequent provisions. Since 1993, SEI/ASCE 7, *Minimum Design Loads and Associated Criteria for Buildings and Other Structures*, has recognized the ductility of EBFs with a response modification factor, R, of 8 (ASCE, 1993; Hines and Jacob, 2010).

While EBFs have been in the AISC *Seismic Provisions* for three decades, they are rarely used in U.S. practice, partly because buckling restrained braced frames (BRBFs) have filled the need for highly ductile braced frames. BRBFs provide high stiffness and ductility (R = 8), solving the main problem that EBFs were developed to address, with less complicated design and detailing and lower overall cost.

However, BRBFs do not have the architectural flexibility of EBFs. AISC *Seismic Provisions* currently restrict the eccentricities that are permitted in BRBFs to be less than a beam depth (AISC, 2022a), so BRBFs can only be used in essentially concentric configurations. When

Chao-Hsien Li, Senior Research Engineer, CoreBrace, LLC, West Jordan, Utah. Email: chaohsien.li@corebrace.com

Paul W. Richards, Associate Professor, Brigham Young University, Provo, Utah. Email: paul.richards@byu.edu (corresponding)

Brandt W. Saxey, Technical Director, CoreBrace, LLC, West Jordan, Utah. Email: brandt.saxey@corebrace.com

Heidi L. Richards, Student Research Assistant, Brigham Young University, Provo, Utah. Email: lynnhi@student.byu.edu

Paper No. 2024–18R

project architecture requires eccentricity greater than a beam depth, additional columns can be added to the BRBFs to make the design compliant with current AISC *Seismic Provisions* [see Figure 1(a) for a project example], but these added columns affect the cost and architecture, making it desirable to have a better alternative.

While the current AISC *Seismic Provisions* (2022a) permit eccentricities up to a beam depth in BRBFs, they do not explicitly define the "eccentricity." Different engineers may use different measures to determine the amount of eccentricity. As illustrated in Figure 1(b), some engineers use the vertical offset—denoted as e_v—measured from the beam centerline to the brace-to-brace or brace-to-column intersection. On the other hand, some designers prefer the horizontal offset e_h measured from a brace-to-beam intersection to the adjacent column centerline or to the beam midspan point. In this paper, e_h is utilized to define the bracing eccentricity in a BRBF for the ease of deriving the design equations for force demands on beams. Additionally, defining eccentricity horizontally aligns with the approach used for EBFs, though for EBFs, the clear eccentricity represents the actual range of the yield zone. In contrast, the centerline-to-centerline eccentricity is suggested for BRBFs because it is more practical for calculating force demands in the elastic design of BRBF beams. Furthermore, as shown in Figure 1(b)-top, the horizontal bracing eccentricities (denoted as e_{hL} and e_{hR} for the e_h to left and right of the beam midspan, respectively) in a chevron (inverted-V) braced frame can be unequal between the two sides of the beam midspan. However, this research focuses on the potentially common case where the bracing eccentricities are equal at both sides of the beam midspan (i.e., $e_{hL} = e_{hR}$).

This research investigates the design and performance of BRBFs with greater eccentricities than are currently permitted. BRBFs with eccentricities are not EBFs because they are designed for different intended plastic mechanisms as illustrated in Figure 2. In a BRBF with eccentricity, the braces are designed to yield and to serve as the main structural fuses, and the other members, including the columns and all regions of beams, are intended to remain elastic. The eccentricity is accounted for when designing the BRBF beam to ensure it remains elastic. By contrast, in an EBF, the beam is designed to yield at the link portion while other components remain essentially elastic. For the chevron BRBFs with eccentricity [Figure 2(a)] investigated in this study, each beam was assumed to be a pin-ended continuous member. For the single-diagonal BRBFs with eccentricity investigated in this study, each beam was assumed to be composed of two separate members (or segments): stub and beam [Figure 2(b)]. The stub is the member accommodating the eccentricity and is rigidly connected to the adjacent column, while the beam member is a pinned beam element placed between the stub and the column away from the stub. In this eccentric BRBF configuration, the stubs and the adjacent columns constitute an elastic half moment resisting frame (half-MRF), and the half-MRF columns would partially resist the story shears when the BRBF is subjected to lateral forces.

While conventional design practice neglects the lateral stiffness of the half-MRF and assumes the braces take total story shears for conservative brace sizing, this study incorporates the half-MRF stiffness into brace sizing to achieve a more economical design. Another design issue with the single-diagonal BRBFs with eccentricities is that the columns in the half-MRF may experience higher moment demands than the columns in concentric BRBFs. For simplicity, the half-MRF columns are treated as typical BRBF columns, with seismic moment demand neglected, as permitted by the AISC *Seismic Provisions* (2022a), in the case study designs presented in this paper. The effects of seismic

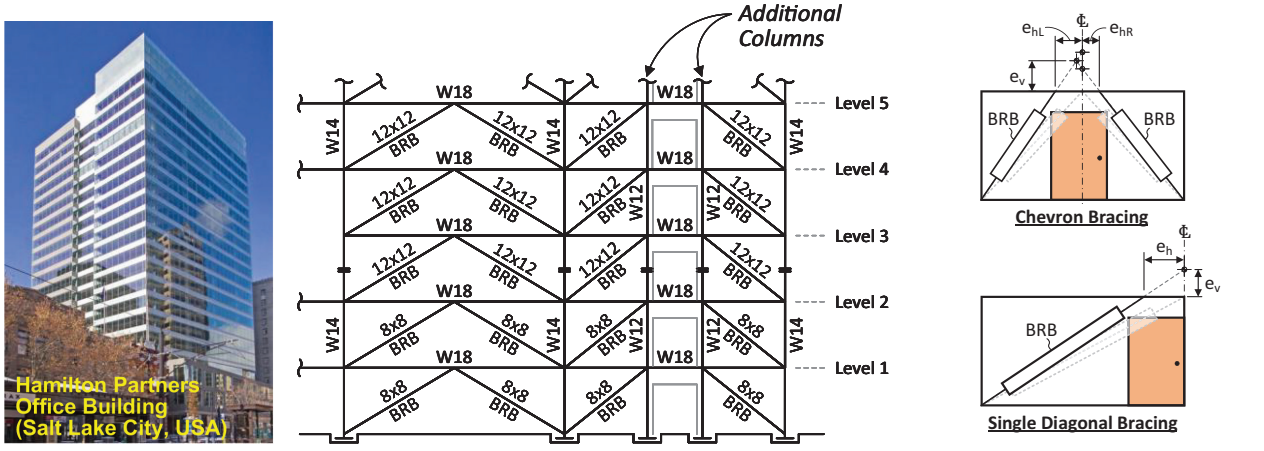

(a) Picture and elevation *(b) Bracing eccentricity definitions*

Fig. 1. BRBF project where additional columns were added to address the architectural constraints.

moment demand on the design of the half-MRF columns will be discussed in the companion paper.

It is worth noting that, as shown in Figure 2, this study chooses the eccentric BRBFs with pin connections at the beam ends as the subjects to investigate because these configurations represent the least-stiff cases. In practice, these pin connections in the beams could be replaced by the moment connections, which could provide additional lateral resistance. In Figure 2(b), the nonalternating configuration is used for the single-diagonal BRBFs because this configuration can accommodate a corridor in the same location at each of the different floor levels. In addition, the nonalternating, single-diagonal bracing configuration represents a more challenging case for design of BRBF beams as the beams are subjected to higher axial forces as compared to the alternating single-diagonal BRBF. Thus, the feasibility of the nonalternating case proven by this study can be extended to the alternating case.

Prinz and Richards (2012) first proposed using BRBFs with eccentricities and investigated frames in the single-diagonal bracing configuration, comparing their design and performance with EBFs. Twelve BRBFs were designed with different story heights (three, six, and nine), two bay widths, and two strength levels. Response history analysis confirmed that frame yielding was confined to the braces. Maximum drifts were less than 2%, and residual drifts were less than 0.5% under design-level shaking. However, a comparison of frame weights indicated the BRBFs with eccentricities were 40% to 100% heavier than EBFs with comparable strength, largely due to a conservative design procedure for the BRBF columns. A subsequent economic analysis of the same frames by Vayda (2015) found that the savings in detailing and fabrication for those BRBFs with eccentricities was not sufficient to offset the higher material costs. It is noted that the previous studies assumed a conventional design approach, where braces in a BRBF are sized for total story shears. This research, however, accounts for the contribution of the half-MRF in single-diagonal BRBFs with eccentricities in resisting part of the story shear, leading to a refined evaluation of brace force demands and more economical design.

Other studies have investigated more economical BRBFs with eccentricities that had two-brace-per-bay (i.e., chevron-type) configurations. Lejano and Mas (2017) investigated BRBFs with a range of eccentricities (0.1 to 0.9 of the beam length) and a variety of brace configurations (one brace per bay, V, inverted V). The designs and pushover analyses indicated that eccentricities greater than 0.4 of the beam length required exceptionally large braces to meet drift limits. Shakib and Safi (2012) compared BRBFs with eccentricity and EBF performance from response history analysis (RHA) and identified cases (story height/ground shaking intensity) when each had the lower story drift. Hosseini and Amiri (2017) compared the collapse potential of buildings with either EBF or BRBF with eccentricity.

This study investigates the seismic design and performance of BRBFs with eccentricities and is presented in a two-part paper. This paper, constituting Part 1, first describes the design procedures for the eccentric BRBFs in chevron and single-diagonal configurations. Analysis methods for determining force demands in braces, beam, and columns are presented. Subsequently, the design considerations and results for nine case study buildings are described. The designs show the impact that eccentricities have on member sizing and overall frame weight. The accompanying paper, Part 2 (Li et al., 2026), presents the nonlinear analysis studies, including response history

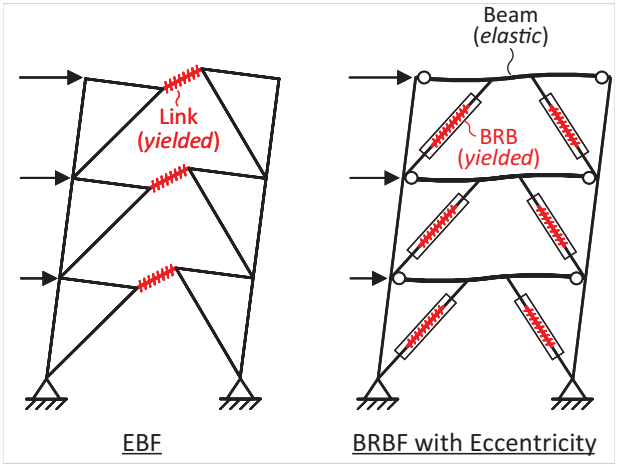

(a) Chevron bracing configuration

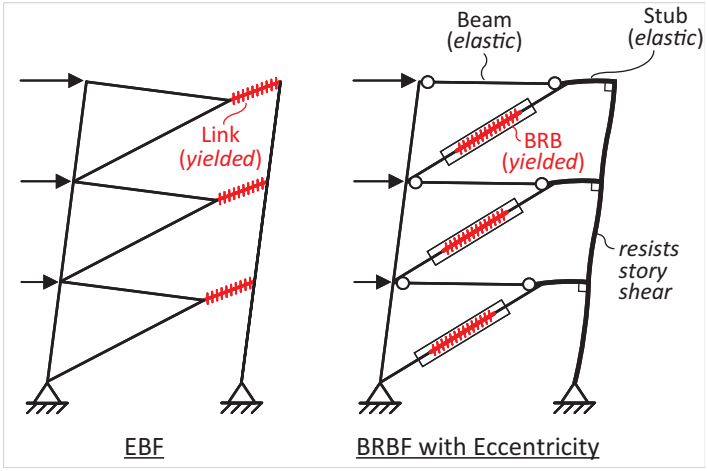

(b) Single-diagonal bracing configuration

Fig. 2. Different intended plastic mechanism for BRBFs with eccentricity as compared to EBFs.

analyses and pushover analysis, for evaluating the seismic performance of these nine case study designs and the design implications.

SEISMIC DESIGN OF ECCENTRIC BRBFS

Overview and Brace Design

The brace design procedures for BRBFs with eccentricity are the same as for concentric BRBFs. The braces are sized to remain elastic under the axial force demands resulting from the design seismic force effects, which can be determined from the equivalent lateral force (ELF) procedure or modal response spectrum analysis (MRSA) (ASCE, 2022). Additionally, the braces are checked to ensure they provide enough stiffness to satisfy drift requirements.

Figure 3 illustrates the effect of increasing brace eccentricity on elastic behavior of chevron BRBFs under lateral forces. Assuming the braces take the entire story shear in the BRBF, the brace axial force (P_{br}) increases with eccentricity because of the change in brace angle, leading to an increase in brace core area. Despite increasing brace core areas, the BRBF lateral stiffness, K_f, generally decreases with eccentricity due to the inefficiency of the braces in providing lateral stiffness resulting from the steeper angle and the larger beam flexural deflection. The trend of decreasing BRBF lateral stiffness with eccentricity implies that the brace design may be governed by drift when the eccentricity is large.

Figure 4 illustrates the effect of increasing brace eccentricity on single-diagonal BRBFs. It is noted that when the eccentricity exists, the half-MRF, composed of the stubs and the adjacent columns, resists partial story shear. As derived in Part 2 (Li et al., 2026), the fraction of story shear carried by the half-MRF column can be approximated by the ratio of the eccentricity to the BRBF span width, e/L, while the brace carries approximately $(1 - e/L)$ of the total story shear. Hence, as the eccentricity increases, the column shear, V_c, increases and the story shear taken by the braces, V_{br}, decreases, which tends to reduce the brace axial force, P_{br}. However, the steeper brace angle tends to increase P_{br}. Combined, the first effect is greater than the second, and P_{br} tends to decrease with eccentricity. Thus, the brace core area can be decreased with the brace eccentricity. Although the decreasing core area and steeper brace angle decrease the lateral stiffness provided by the brace when the eccentricity increases, the participation of the half-MRF increases with eccentricity. The analysis results in this study show that the net effect of these two actions tends to make the total frame lateral stiffness, K_f, slightly increase with the eccentricity for the single-diagonal eccentric BRBFs. It is worth noting that the effects of increasing eccentricity mentioned earlier are based on considering the contribution of the half-MRF in resisting story shear in the design of single-diagonal BRBFs, as this research explores the economy of this BRBF type. In contrast, neglecting the lateral stiffness of the half-MRF would result in a more conservative brace design, leading to an increase in brace core area with eccentricity (due to the steeper brace angle) in single-diagonal BRBFs.

Capacity Design: General

After the braces are sized using ELF or MRSA methods, the BRBF beams and columns are sized using capacity design concepts. This approach considers the maximum possible forces that could be generated in the braces and ensures that the beams and columns remain elastic under the force demands induced by these brace forces.

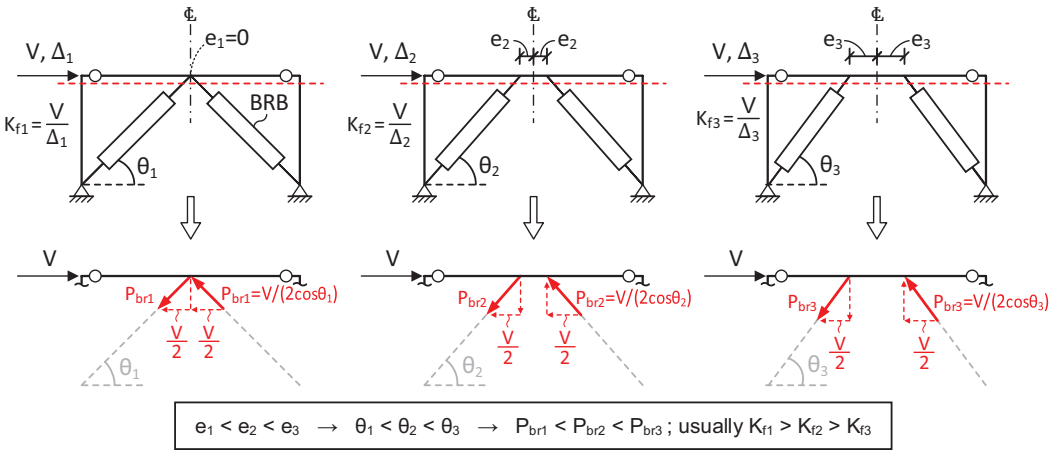

Fig. 3. Effects of increasing bracing eccentricity on elastic behavior of chevron BRBFs.

The maximum possible brace axial forces used in capacity design are estimated from the code-prescribed adjusted brace strengths (AISC, 2022a). The equations for the adjusted brace strengths in tension and compression, denoted as P_{uT} and P_{uC}, are:

$$P_{uT} = \omega F_{ysc} A_{sc} \tag{1}$$

$$P_{uC} = \omega \beta F_{ysc} A_{sc} \tag{2}$$

where ω is the strain-hardening adjustment factor and β is the compression strength adjustment factor (AISC, 2022a); A_{sc} is the area of steel core; and F_{ysc} is the actual yield stress, determined from a coupon test or estimated as $R_y F_y$, where R_y is the ratio of the expected yield stress to the specified minimum yield stress and F_y is the specified minimum yield stress.

The beam capacity design accounts for the effects induced by the adjusted brace strengths of the braces. In V and chevron (inverted-V) bracing configurations, unbalanced forces between the tensile and compressive braces affect the shear and flexural demands on the beams. For column capacity design, the cumulative effects of simultaneous yielding and development of adjusted strengths for all braces in a BRBF are considered.

Capacity Design of Beams

This section presents the determination of force demands for capacity design of beams in eccentric BRBFs. Design considerations for the chevron and single-diagonal bracing cases are discussed separately.

Chevron-Type Configurations

Figure 5 shows the determination of capacity-limited seismic effects, E_{cl}, in beams in chevron eccentric BRBFs (V configurations similar). As shown in Figure 5(b), each beam is divided into three regions for determining the force demands. Regions 1 and 3 refer to the exterior beam regions connected to columns, where Region 3 is the one attached to the column that experiences compression from the lateral forces (Figure 5). The interior portion is defined as Region 2. For clarity, Regions 1, 2, and 3 are abbreviated as R1, R2, and R3 in the subscripts of the corresponding symbols.

The chevron configuration in this paper represents BRBFs with beams that are pin connected at or near the columns. In such cases, as illustrated in Figure 5(c), the E_{cl} forces in each beam can be analyzed by using a simple beam model subjected to a pair of adjusted brace strengths, P_{uT} and P_{uC}, coming from the braces underneath the beam. The vertical components of brace forces induce the shear and moment demands in the beam [Figure 5(c)-left]. The equations for computing E_{cl} shear forces in Regions 1, 2, and 3 (designated as $V_{Ecl,R1}$, $V_{Ecl,R2}$, and $V_{Ecl,R3}$, respectively) are obtained:

$$V_{Ecl,R1} = \frac{(b+2e)P_{uT}\sin\theta - bP_{uC}\sin\theta}{2b+2e} \tag{3}$$

$$V_{Ecl,R2} = -\left(\frac{b}{2b+2e}\right)(P_{uT}\sin\theta + P_{uC}\sin\theta) \tag{4}$$

$$V_{Ecl,R3} = \frac{(b+2e)P_{uC}\sin\theta - bP_{uT}\sin\theta}{2b+2e} \tag{5}$$

where θ is the brace inclination angle measured from the horizontal, e is the horizontal eccentricity between the beam midspan and brace-to-beam intersection, and b is the span of exterior beam regions for the case where R1 and R3 are equal in length. In preliminary design, locations of

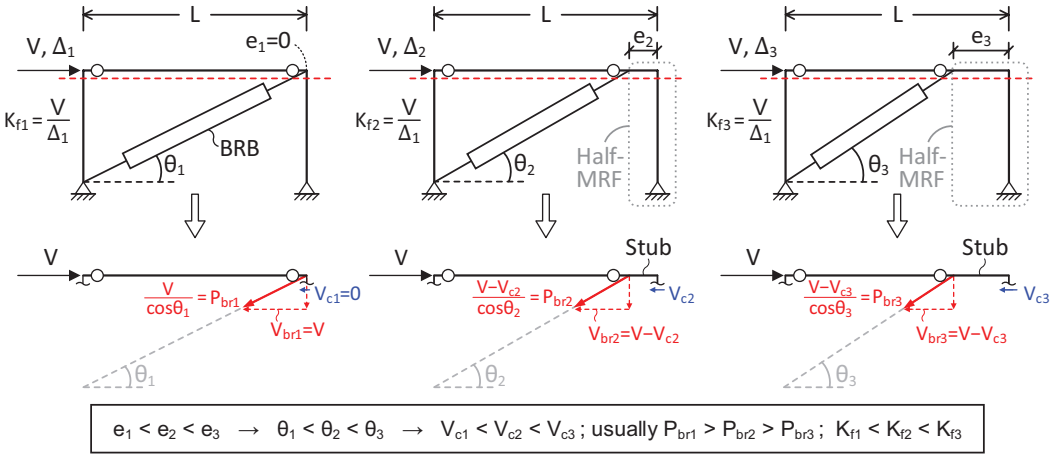

Fig. 4. Effects of increasing brace eccentricity on elastic behavior of single-diagonal BRBFs.

pin connections at the beam ends are assumed to be at the column centerline for simplicity. Note that the positive sign of a shear indicates that the shear causes clockwise rotation of beam elements. As demonstrated in the shear diagram in Figure 5(c)-left, a significant shear force is induced in the interior beam region and acts in the opposite direction to the relatively moderate shears developed in the exterior regions. Due to the imbalance of brace forces P_{uT} and P_{uC}, the shear forces in the two exterior regions are unbalanced as well, and the reactions are opposite directions from each other. Region 3 takes a higher shear than Region 1.

Figure 5(c)-left also presents the E_{cl} moment diagram in the beam. The maximum moments in the Regions 1 and 3 (designated as $M_{Ecl,R1}$ and $M_{Ecl,R3}$, respectively) can be calculated from:

$$M_{Ecl,R1} = V_{Ecl,R1} b = \frac{b(b+2e)P_{uT}\sin\theta - b^2 P_{uC}\sin\theta}{2b+2e} \quad (6)$$

$$M_{Ecl,R3} = -V_{Ecl,R3} b = -\left[\frac{b(b+2e)P_{uC}\sin\theta - b^2 P_{uT}\sin\theta}{2b+2e}\right] \quad (7)$$

As usual, the positive sign for moment indicates concavity upward. Note that the unbalanced shears between the Regions 1 and 3 cause the unbalanced moments between these two regions. Region 3 resists a higher flexural demand. Further, the moment demands $M_{Ecl,R1}$ and $M_{Ecl,R3}$ are also the end moments of the Region 2, and the large one, $M_{Ecl,R3}$, is taken as the governing moment demand for the Region 2.

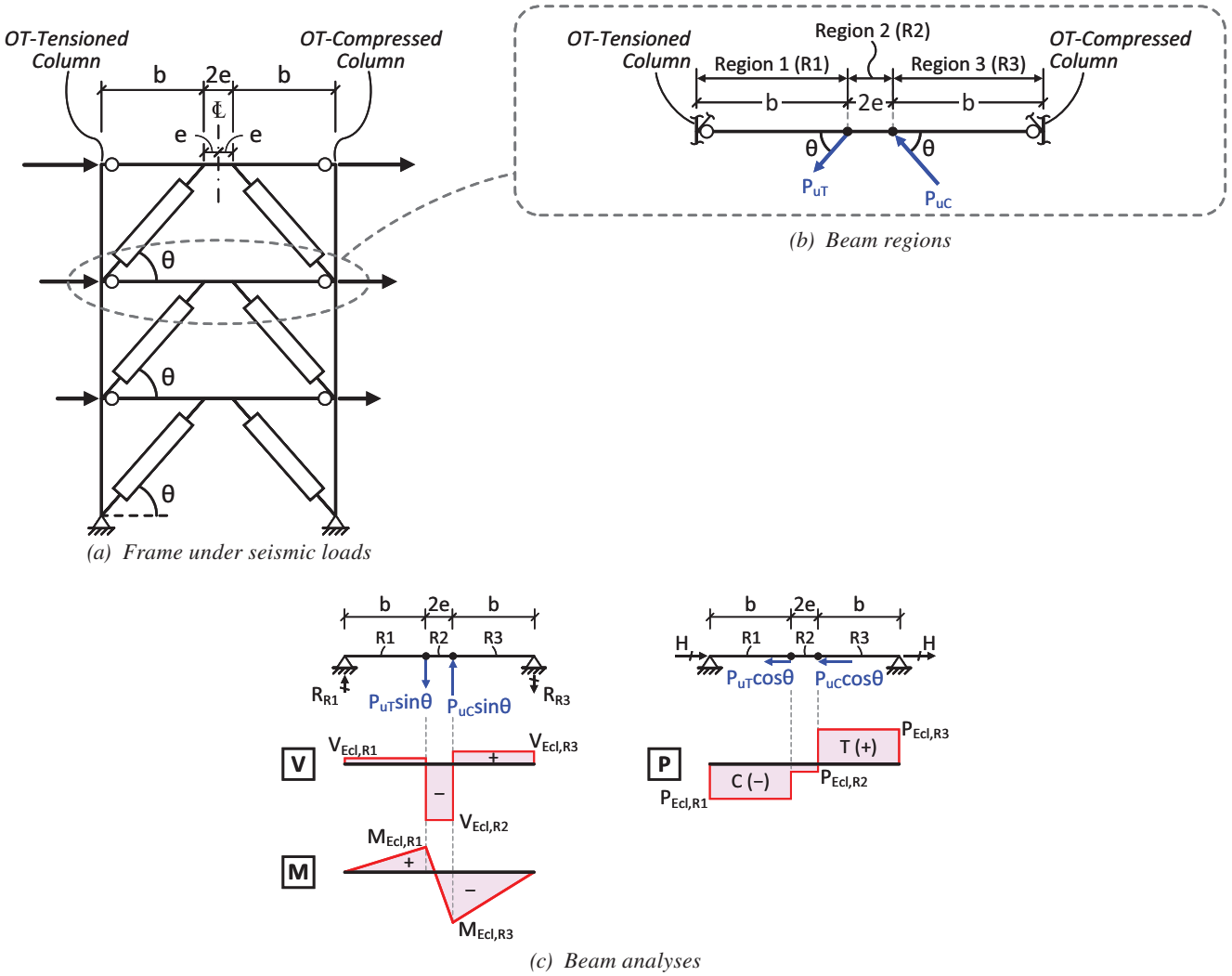

Fig. 5. Estimation of capacity-limited seismic demands in chevron eccentric BRBF beams.

These procedures capture the shear and moment in a centerline model of the beam. The local and global force issue in the concentric chevron braced frame presented in Fortney and Thornton (2017) may require additional consideration, but it is expected that local effects will be small compared to the centerline forces when the brace eccentricity exists. The adequacy of the current procedure for the case study designs can be seen in the FEM analysis presented in Part 2 (Li et al., 2026).

Figure 5(c)-right illustrates the determination of the E_{cl} axial forces. The horizontal components of the adjusted brace strengths, P_{uT} and P_{uC}, are applied on a simple beam model with horizontal reactions, representing the resultant horizontal external forces delivered to each end of the beam. The external forces include the collector force and the horizontal component of brace force coming from the upper story. In real applications, the ratio between the inertial forces delivered to two ends of the beam is dependent on the collector length and tributary seismic mass on each side of the beam. In this study, it is simply assumed that identical reactions, H, act at both ends of the beam model [Figure 5(c)-right], essentially representing the case where the tributary seismic mass to each side of the BRBF are identical. Thus, the E_{cl} axial forces in Regions 1, 2, and 3 (designated as $P_{Ecl,R1}$, $P_{Ecl,R2}$, and $P_{Ecl,R3}$, respectively) are estimated as:

$$P_{Ecl,R1} = -H = -\left(\frac{P_{uT}\cos\theta + P_{uC}\cos\theta}{2}\right) \tag{8}$$

$$P_{Ecl,R2} = H - P_{uC}\cos\theta = -\left(\frac{P_{uC}\cos\theta - P_{uT}\cos\theta}{2}\right) \tag{9}$$

$$P_{Ecl,R3} = H = \frac{P_{uT}\cos\theta + P_{uC}\cos\theta}{2} \tag{10}$$

As shown in the obtained axial force diagram [Figure 5(c)-right], the seismic effect would cause Regions 1 and 3 to resist significant compressive and tensile axial forces, respectively, while inducing relatively small compressive force in the Region 2.

As shown in Figure 6, the total force demands [Figure 6(a)] in the chevron eccentric BRBF beams come from the superposition of seismic [Figure 6(b)] and gravity [Figure 6(c)] effects. In general, the interior beam region (Region 2) is subjected to high shear and moment and moderate axial force, while the two exterior regions (Regions 1 and 3) are in significant combined axial and bending. This indicates that the design of a chevron beam may be governed by either combined axial and shear (i.e., *P-V* interaction) demands in the interior region, or combined axial and bending (i.e., *P-V* interaction) demands in the exterior regions. For the shear and moment demands, the gravity effect counteracts the seismic effect in Region 3, whereas

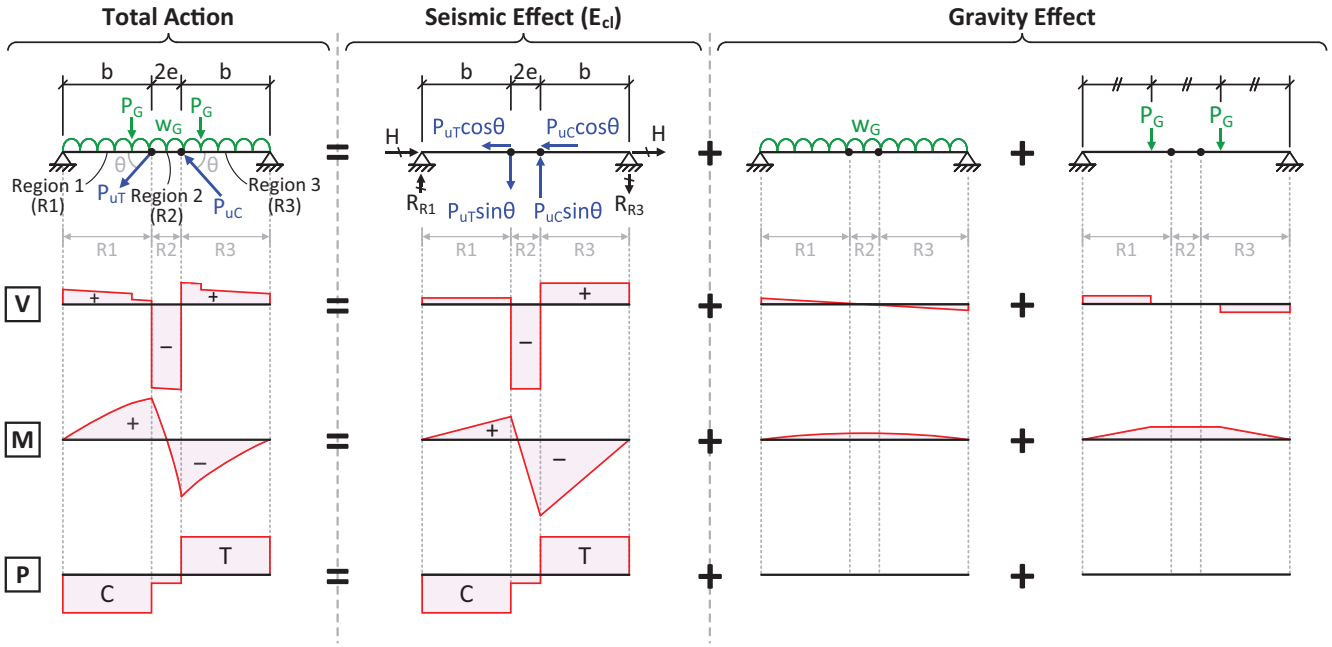

(a) Total from superposition *(b) Seismic effects* *(c) Gravity effects*

Fig. 6. Chevron eccentric BRBF beam design forces.

the two effects are additive in Region 1. As a result, the presence of gravity loads would make the seismic-induced unbalance in shear and moments between the two exterior regions less significant. Considering that seismic effects are usually much more intensive than gravity effects in typical buildings, it is expected that Region 3 generally takes higher total demands in shear and moment compared to Region 1. However, since Region 1 is subjected to compression while Region 3 is in tension, Region 1 has a lower axial capacity. It is hard to pre-judge which one of these two exterior regions represents the more critical case. As such design checks must be conducted for all three regions.

In accordance with strength design load combinations 6 and 7 from SEI/ASCE 7, Section 2.3 (ASCE, 2022), the governing total moment demand, M_u, which accounts for combined seismic and gravity effects and is used for the *P-M* interaction check for each beam region, will be the greater of the following two:

$$M_u = B_1\left[(1.2+0.2S_{DS})M_D + f_L M_L\right] + M_{Ecl} \tag{11}$$

$$M_u = B_1\left[(0.9-0.2S_{DS})M_D\right] + M_{Ecl} \tag{12}$$

where M_D and M_L are the moments due to dead load and live load, respectively. M_{Ecl} is the moment demand due to the E_{cl} effect. S_{DS} is the design spectral response acceleration parameter at short periods. The load factor for live load, f_L, defaults to 1.0 but is permitted to be reduced to 0.5 when the unreduced live load does not exceed 100 psf. B_1 is the multiplier factor, as stipulated in AISC *Specification* Appendix 8 (2022b), to account for the *P*-δ effect for the beam regions in compression (i.e., Regions 1 and 2). For Region 3, which is in tension, $B_1 = 1.0$. Similarly, the governing total shear demand, V_u, used for the *P-V* interaction check for each beam region will be the greater of the following two:

$$V_u = (1.2+0.2S_{DS})V_D + f_L V_L + V_{Ecl} \tag{13}$$

$$V_u = (0.9-0.2S_{DS})V_D + V_{Ecl} \tag{14}$$

Nonalternating Single-Diagonal Configuration

Due to the asymmetry of the braced frames in single-diagonal bracing configurations, the brace frame behavior varies with the direction of seismic forces. Two analysis cases must be considered separately in the capacity design of single-diagonal BRBFs regardless of concentric or eccentric frame. As shown in Figure 7(a), Analysis Case 1 is defined as the case where the seismic loading causes the braces to be in tension. Figure 8(a) shows Analysis Case 2, where the seismic forces cause the braces to be in compression. Figures 7(b) and 8(b) illustrate the brace forces considered for determining the E_{cl} effects on the beam in a typical floor for Analysis Cases 1 and 2, respectively. The characters *U* and *L* used in the symbols $P_{uT,U}$, $P_{uT,L}$, $P_{uC,U}$, and $P_{uC,L}$ represent the brace forces with adjusted strength (P_{uT} or P_{uC}) coming from the upper and lower stories of the beam, respectively. For the beam at the top level of a BRBF, there is no brace force ($P_{uT,U}$ or $P_{uC,U}$) coming from the upper story, and similarly at the lowest level of a BRBF (at the base plate), there is no brace force ($P_{uT,L}$ or $P_{uC,L}$) coming from the lower story.

Figures 7(c) and 8(c) illustrate the beam analyses and resulting beam actions for Analysis Cases 1 and 2, respectively. Note each BRBF beam is composed of two members: stub and beam. A beam model having one end simply supported and the other end fixed is used. An inner hinge is placed in the beam model to represent the pin connection between the beam and stub. In the preliminary design, the hinge can simply be set at the brace-to-beam intersection point. Likewise, the beam member length *b* can be taken as the distance measured from the column centerline to the brace-to-beam intersection point.

For Analysis Case 1 [Figure 7(c)-left], the vertical component of tensile brace force from the lower-story subjects the cantilever beam-like stub member to negative bending, while the beam member (beyond the stub) does not resist any shear and moment due to the seismic effect. The seismic shear and moment at the stub's fixed end, denoted as $V_{Ecl1,Stub}$ and $M_{Ecl1,Stub}$, respectively, can be estimated as:

$$V_{Ecl1,Stub} = -P_{uT,L}\sin\theta \tag{15}$$

$$M_{Ecl1,Stub} = -e\left(P_{uT,L}\sin\theta\right) \tag{16}$$

Note that the subscript *Ecl*1 represents the capacity-limited seismic effect, E_{cl}, in Analysis Case 1. As shown in Figure 7(c)-right, to analyze the seismic axial demand in the beams in single-diagonal BRBFs, the horizontal components of the braces forces coming from both upper and lower stories are considered. For simplicity, an identical reaction force, *H*, is assumed at both ends of the beam model to represent the case that the collector forces delivered to each side of the beam are identical. The E_{cl} axial forces induced in stub and beam (denoted as $P_{Ecl1,Stub}$ and $P_{Ecl1,Beam}$, respectively) can be estimated as:

$$P_{Ecl1,Stub} = \frac{(P_{uT,L}\cos\theta - P_{uT,U}\cos\theta)}{2} \tag{17}$$

$$P_{Ecl1,Beam} = -\frac{(P_{uT,L}\cos\theta + P_{uT,U}\cos\theta)}{2} \tag{18}$$

For Analysis Case 2 [Figure 8(c)], brace forces are compressive, subjecting the stub to positive bending and moderate compressive force, while significant tensile force is induced in the beam member. The equations for estimating the critical member forces in the beam are as follows:

$$V_{Ecl2,Stub} = P_{uC,L} \sin\theta \tag{19}$$

$$M_{Ecl2,Stub} = e(P_{uC,L} \sin\theta) \tag{20}$$

$$P_{Ecl2,Stub} = -\frac{(P_{uC,L} \cos\theta - P_{uC,U} \cos\theta)}{2} \tag{21}$$

$$P_{Ecl2,Beam} = \frac{(P_{uC,L} \cos\theta + P_{uC,U} \cos\theta)}{2} \tag{22}$$

where the subscript *Ecl*2 used in the symbols represents the E_{cl} effects in Analysis Case 2.

Figures 9 and 10 illustrate the superposition of the seismic and gravity effects on the beams in single-diagonal eccentric BRBFs for Analysis Cases 1 and 2, respectively. As shown in the diagrams of the total force demands [Figures 9(a) and 10(a)], in general, the stub is subjected to high shear and moment demands alongside moderate axial load, while the beam member resists significant axial load accompanied with relatively low flexural demand. For a complete design, both stub and beam need to be checked with *P-V* and *P-M* interaction demands developed in Analysis Cases 1 and 2. The general equations for computing the total moment demand (Eqs. 11 and 12) and total shear demands (Eqs. 13 and 14) are applied to both beam and stub members. Note that the beam member is in compression in Analysis Case 1 while resisting tensile force in Analysis Case 2. The flexural demand in the beam member, which is due to the gravity effect only, remains the same in both scenarios. Thus, the design of the beam member would be generally governed by the *P-M* interaction demands in Analysis Case 1.

On the other hand, it is hard to prejudge which analysis case would govern the design of stub. In Analysis Case 1,

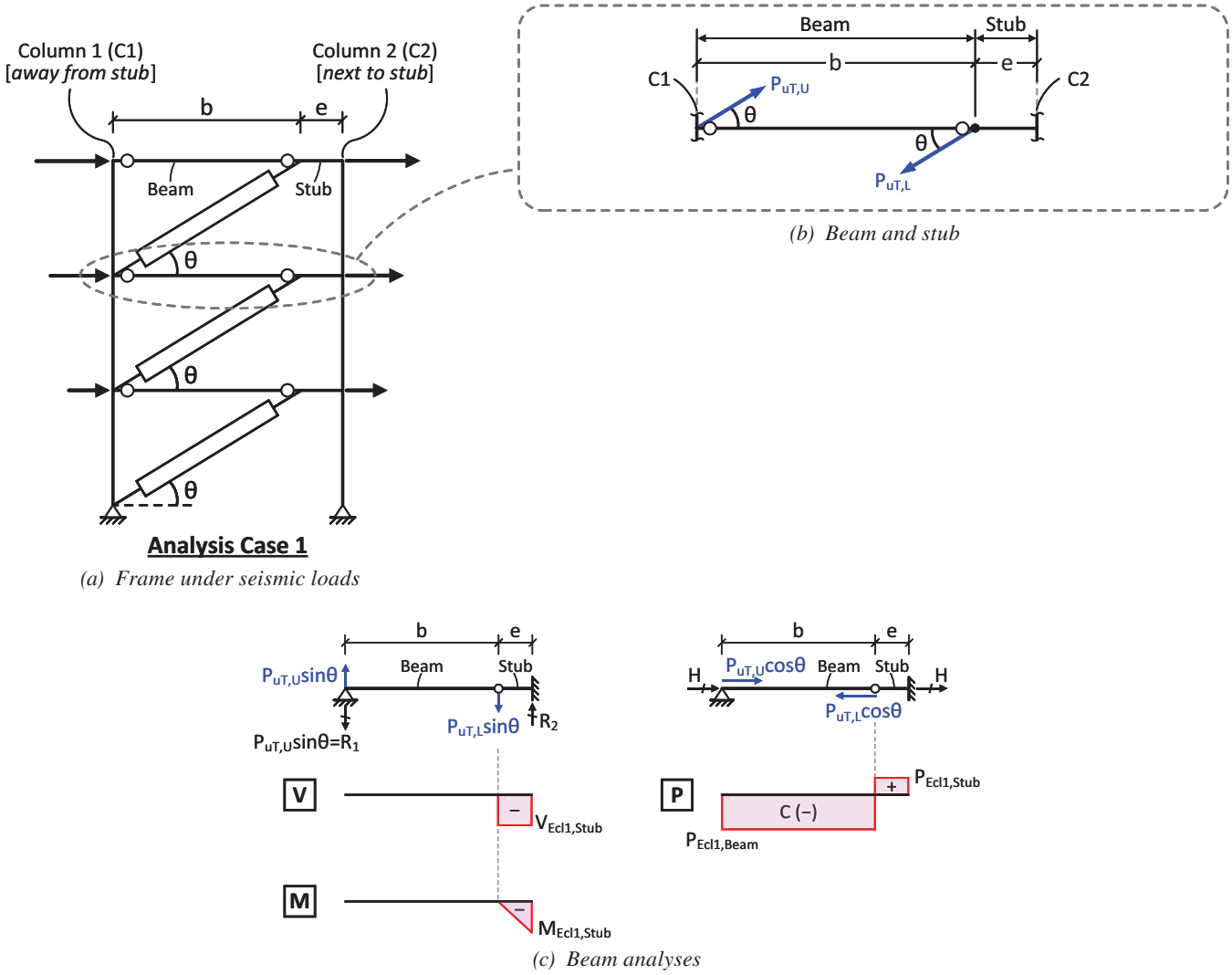

(a) *Frame under seismic loads*

(b) *Beam and stub*

(c) *Beam analyses*

Fig. 7. Estimation of capacity-limited seismic demands on beams in single-diagonal eccentric BRBFs in Analysis Case 1.

the seismic [Figure 9(b)] and gravity [Figure 9(c)] effects are additive for both shear and moment demands in the stub, whereas these two effects in Analysis Case 2 [Figures 10(b) and 10(c)] counteract with each other. Thus, the magnitudes of the total shear and moment demands induced in the stub in Analysis Case 1 [Figure 9(a)] would be higher than those developed in Analysis Case 2 [Figure 10(a)]. However, the stub is in tension in Analysis Case 1, but in compression in Analysis Case 2. Design checks for the stub must be conducted for both analysis cases.

Capacity Design of Columns

This section presents the determination of force demands for column capacity design in eccentric BRBFs. Design considerations for the chevron and single-diagonal bracing cases are discussed separately.

Chevron-Type Configurations

Figure 11 shows the determination of column axial forces due to the E_{cl} effect for chevron eccentric BRBFs. To estimate the maximum possible axial forces that can be developed in the columns, as shown in Figure 11(a), the plastic mechanism in which all the braces in a multistory braced frame simultaneously yield and develop their adjusted strengths (P_{uT} or P_{uC}) is considered. The resulting column axial forces can be obtained by taking the free-body diagrams [Figure 11(b)] for each side of columns in the braced frame with all the vertical forces, coming from the brace forces and beam end shears, applied on the columns. The sizing of the columns is governed by the axial demand in the overturning (OT)-compressed columns (i.e., the compressed columns under the OT action of the frame) because the seismic and gravity effects are additive. The general

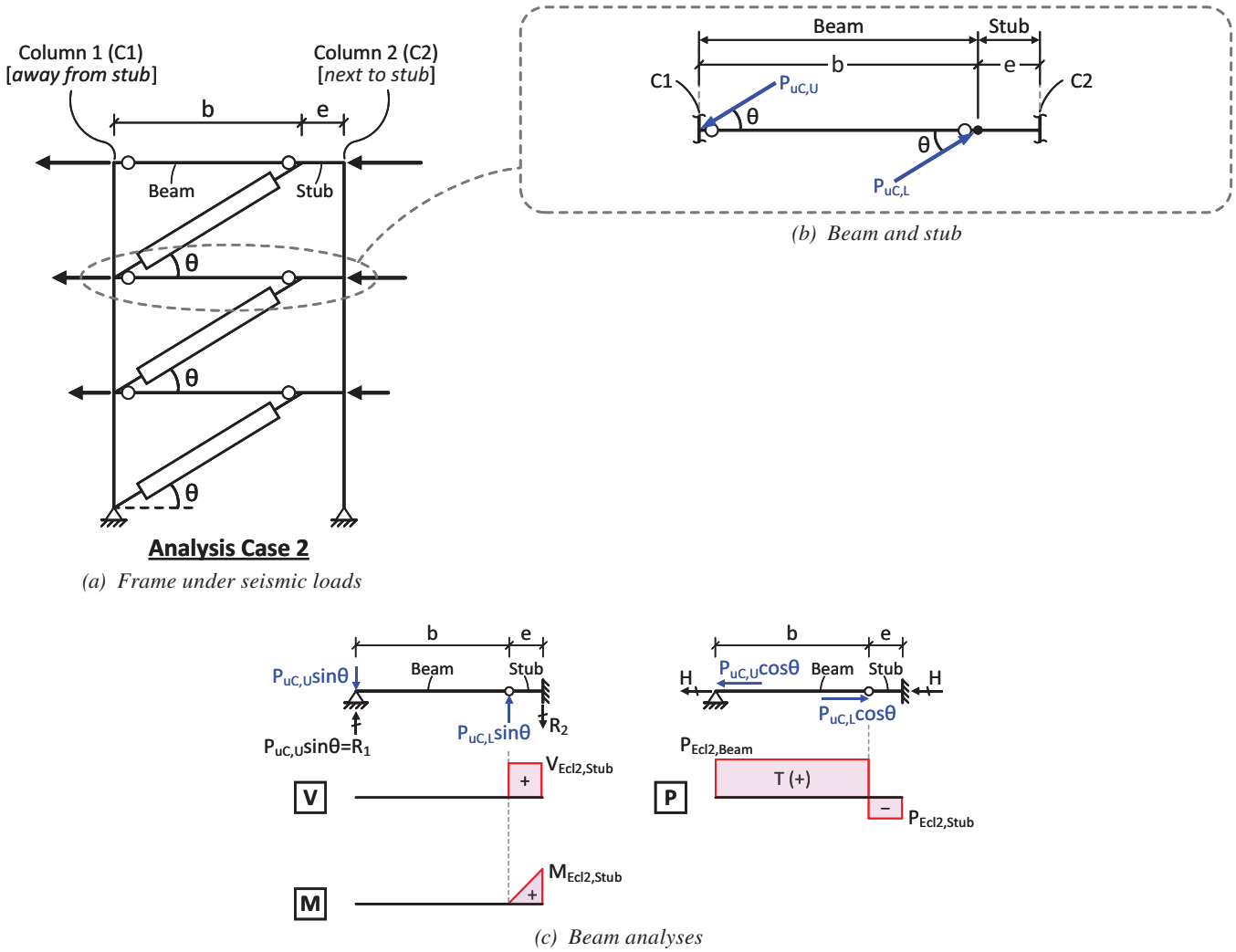

(a) Frame under seismic loads

(b) Beam and stub

(c) Beam analyses

Fig. 8. Estimation of capacity-limited seismic demands on beams in single-diagonal eccentric BRBFs in Analysis Case 2.

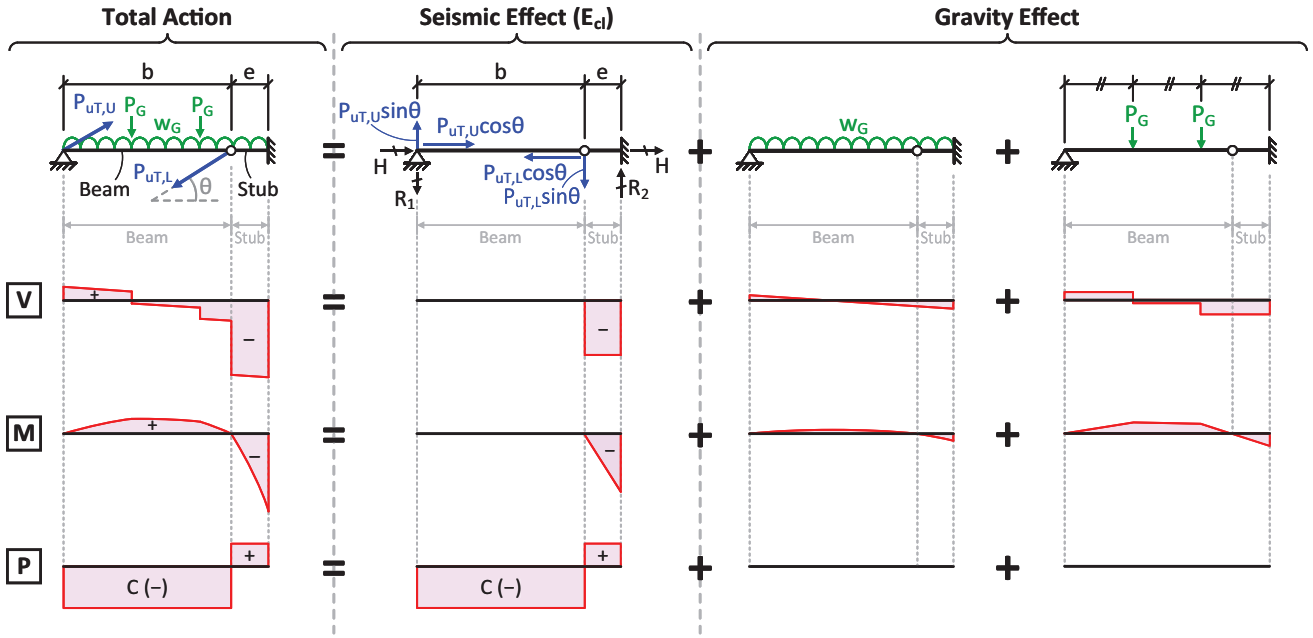

(a) Total from superposition (b) Seismic effects (c) Gravity effects

Fig. 9. Single-diagonal eccentric BRBF beam design forces in Analysis Case 1.

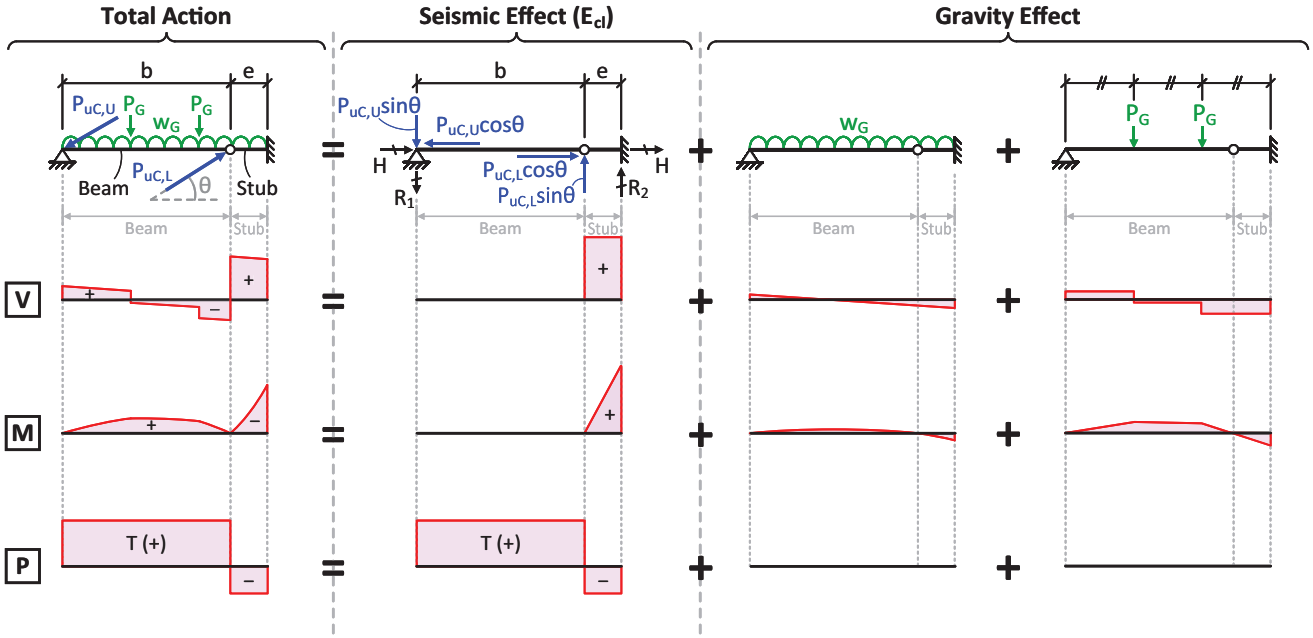

(a) Total from superposition (b) Seismic effects (c) Gravity effects

Fig. 10. Single-diagonal eccentric BRBF beam design forces in Analysis Case 2.

equation for computing the E_{cl} compressive force in the nth-story column, $P_{Ecl,C,n}$, of a N-story chevron eccentric BRBF is:

$$P_{Ecl,C,n} = \sum_{i=n+1}^{N} (P_{uC} \sin\theta)_i - \sum_{i=n}^{N} V_{Ecl,R3,i} \quad (23)$$

where $(P_{uC}\sin\theta)_i = P_{uC,i} \sin\theta_i$ estimates the vertical component of brace force from the ith story; $P_{uC,i}$ and θ_i are the compressive adjusted strength and inclination angle, respectively, for the ith-story braces; and $V_{Ecl,R3,i}$ is the shear in the beam Region 3 (R3) at the ith level, which is computed from Equation 5.

Finally, the total compressive axial force demand P_u, which accounts for the combined gravity and seismic effects is computed from:

$$P_u = (1.2 + 0.2S_{DS})P_D + f_L P_L + P_{Ecl} \quad (24)$$

where P_D and P_L are the axial force due to dead load and live load, respectively.

Nonalternating Single-Diagonal Configuration

Due to the asymmetry of single-diagonal BRBFs, regardless of whether the braces are concentrically or eccentrically oriented, the maximum seismic demands in the two sides of columns are different. In addition, two analysis cases must be considered in column design as shown in Figures 12(a) and 13(a). For discussion purposes, as shown in Figure 12(a), Column 1 is away from the stub, whereas Column 2 is near the stub (connected to it).

For column design, Figure 12(a) shows the considered plastic mechanism for Analysis Case 1, in which all the braces are assumed to yield and develop their tensile adjusted strength, P_{uT}. In this case, C1 members are OT-tensioned (i.e., tensioned under the overturning action of the frame), while C2 members are OT-compressed. By contrast, Figure 13(a) shows the case under Analysis Case 2 loading, where all the braces are assumed to reach the compressive adjusted strength, P_{uC}, and Columns 1 and 2 are OT-compressed and OT-tensioned, respectively. Figures 12(b) and 13(b) illustrate the analyses of the E_{cl} axial forces in the columns for Analysis Cases 1 and 2, respectively. Note that the member sizing of each side of columns is governed by the analysis case where that side of column is OT-compressed because the seismic and gravity effects are additive in producing compressive column forces.

The design of Column 1 is governed by Analysis Case 2 [Figure 13(b)], and the general equation for the E_{cl} compressive force in the nth-story C1 member, $P_{Ecl2,C1,n}$, of a N-story single-diagonal BRBF is:

$$P_{Ecl2,C1,n} = \sum_{i=n+1}^{N} (P_{uC} \sin\theta)_i \quad (25)$$

On the other hand, the design of Column 2 is governed by Analysis Case 1 [Figure 12(b)], and the general equation for the E_{cl} compressive force in the nth-story C2 member, $P_{Ecl1,C2,n}$ is:

$$P_{Ecl1,C2,n} = \sum_{i=n}^{N} \left|V_{Ecl1,Stub,i}\right| = \sum_{i=n}^{N} (P_{uT} \sin\theta)_i \quad (26)$$

where $V_{Ecl1,Stub,i}$ is the shear in the stub at the ith level under Analysis Case 1. Its magnitude (absolute value) equals to the vertical component of brace force in the ith story, $(P_{uT}\sin\theta)_i = P_{uT,i}\sin\theta_i$ where $P_{uT,i}$ is the tensile adjusted strength of ith-story braces.

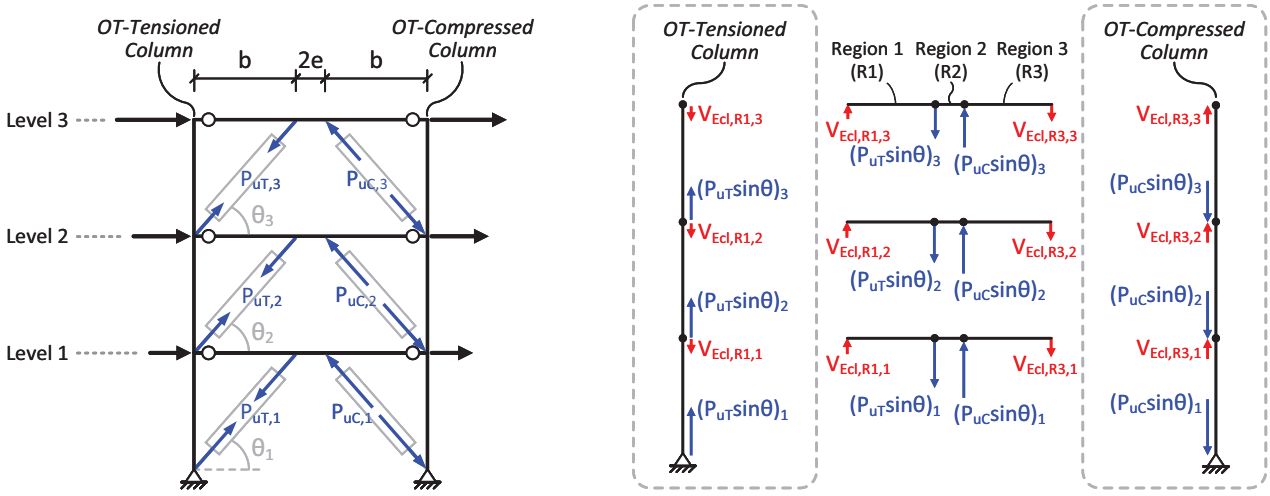

(a) *Frame under seismic loads* (b) *Force diagrams for analysis*

Fig. 11. Estimation of capacity-limited seismic column axial forces in chevron eccentric BRBFs.

By comparing the governing force diagram for determining seismic axial forces in C1 [Figure 13(b)-left] and that for C2 [Figure 12(b)-left], it can be found that, in any story, the C2 member resists one more vertical brace force above that story than the C1 member. This is reflected in the equation for $P_{Ecl1,C2,n}$ (Equation 26) which has a summation starting from the nth story, while the equation for $P_{Ecl2,C1,n}$ (Equation 25) is a summation starting from the $(n + 1)$th story. As a result, the C2 members resist higher seismic axial demand than C1 members. Hence, the two sides of columns in a nonalternating, single-diagonal BRBF may be sized separately to pursue an economical design. Finally, the total compressive axial force, P_u, for sizing the columns is determined per Equation 24, considering the combined gravity and seismic effects.

Furthermore, as shown in Figures 12(b) and 13(b), the stubs would deliver bending moments to the adjacent C2 members because the stubs are moment connected to the C2 members in a single-diagonal BRBF. This moment demand can be significant, especially with large eccentricity. Although the AISC *Seismic Provisions* (2016a) permits neglecting seismic-induced moments in conventional BRBF column design, it is unclear if this relaxation is proper for the single-diagonal BRBFs with eccentricities. For simplicity, the C2 members in the design cases presented later in this Part 1 paper were sized based on axial force demand

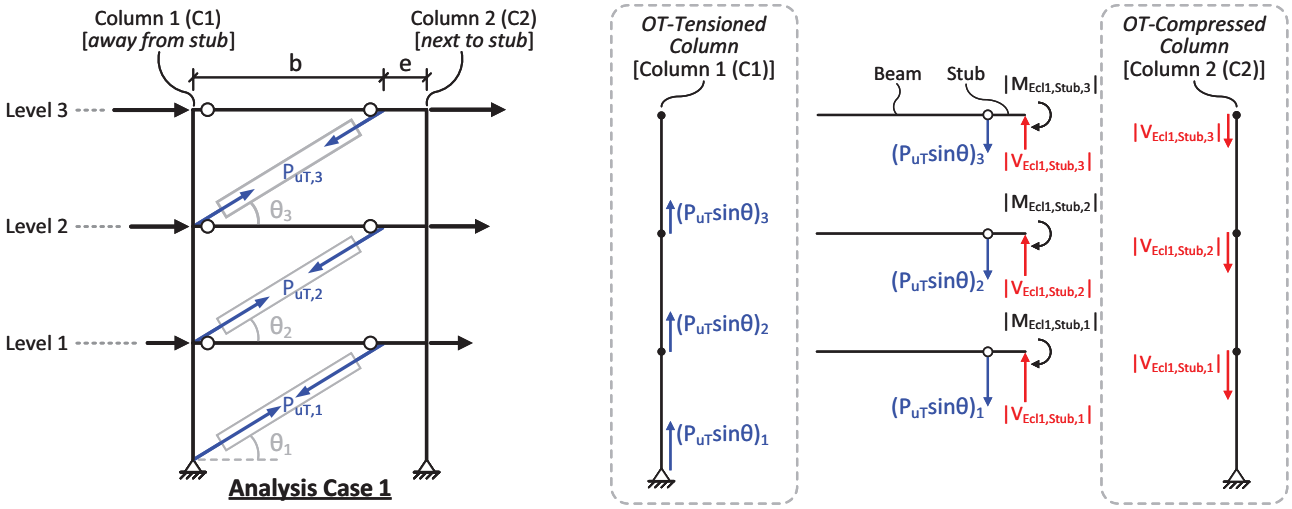

(a) Frame under seismic loads (b) Force diagrams for analysis

Fig. 12. Estimation of capacity-limited seismic column axial forces in single-diagonal eccentric BRBFs in Analysis Case 1.

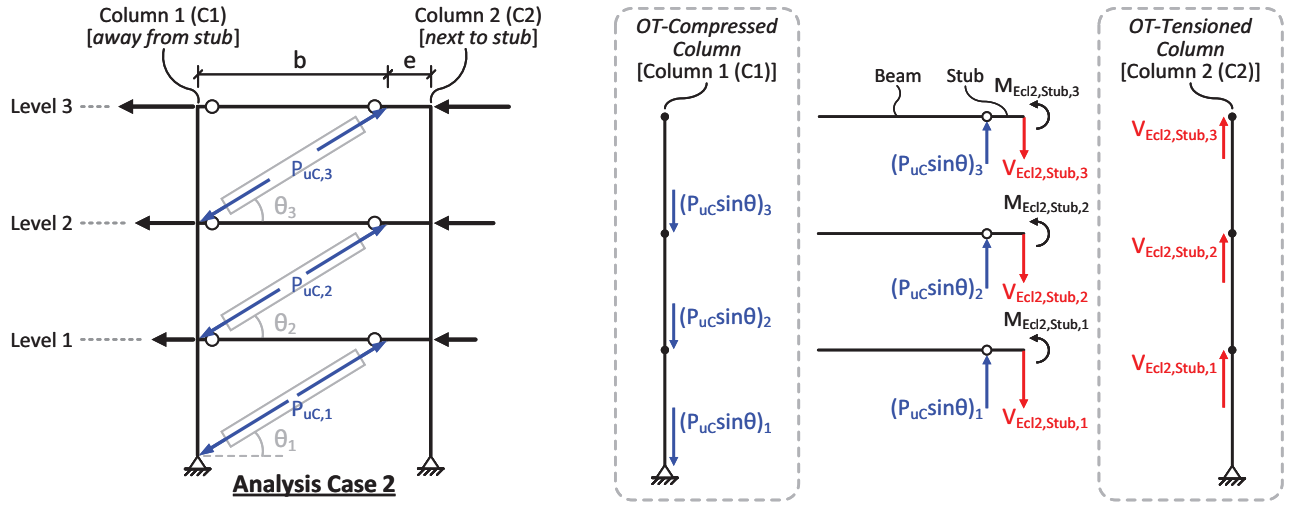

(a) Frame under seismic loads (b) Force diagrams for analysis

Fig. 13. Estimation of capacity-limited seismic column axial forces in single-diagonal eccentric BRBFs in Analysis Case 2.

only, without considering seismic moment demands and with sufficiency verified by the analytical study presented in Part 2 (Li et al., 2026). Further discussion on the performance of BRBFs with C2 members sized with and without consideration of seismic moment demand is also presented in Part 2.

CASE STUDY DESIGNS

Example Buildings Description

Nine BRBF designs representing two building heights (12- and 3-story), two bracing configurations (chevron and single-diagonal), and various eccentricities were developed to investigate the impact of eccentricity on BRBF weight and performance. The buildings were adapted from NIST GCR 10-917-8 (2010). Figures 14(a) and 14(b) show the floor plans for the 12- and 3-story buildings, respectively. The single-bay perimeter BRBF in the longitudinal direction of each building was used for the study, and Figure 15 shows the frame elevations of the nine designs. The designs comply with the 2016 editions of SEI/ASCE 7 (2016), the AISC *Seismic Provisions* (2016a), and the AISC *Specification* (2016b), which were in effect during this study. The buildings were designed for a site with seismic design spectral parameters S_{DS} = 1.0g and S_{D1} = 0.6g and using an importance factor I_e = 1.0 and a deflection amplification factor C_d = 5. The redundancy factor ρ = 1.0 was used, as permitted by SEI/ASCE 7-16 based on the floor plans considered, to avoid oversizing. The buildings, per the NIST report, had a roof dead load of 67 psf, floor dead load of 85 psf, roof live load of 20 psf, and floor live load of 50 psf. The curtain wall weight on the building perimeter was 15 psf.

Based on the number of stories and bracing configurations, as shown in Figure 15, the design cases were divided into four groups: 12S-CH, 12S-SD, 3S-CH, and 3S-SD. The prefixes 12S and 3S mean 12-story and 3-story, respectively, while the suffixes CH and SD represent the chevron and single-diagonal bracing configurations in the BRBFs. In each group, there is one design case with a concentric configuration (Case C) and another design case with braces oriented at an eccentricity, e, equal to 2 times the nominal beam depth (Case E2d). For all design cases, the nominal beam depth (d_b = 21 in.) of W21 beams was used to determine the eccentricity. The E2d cases in each group represent BRBFs with a brace eccentricity that exceeds the code-permitted upper limit (AISC, 2016a). Moreover, in Group 12S-CH, an additional case E1d with e equal to 1 times nominal beam depth was developed. For discussion purposes, each design case is named as its group name added with a suffix representing the eccentricity situation. For example, Design 12S-CH-C represents 12-story chevron BRBFs with concentric braces, while Design 3S-SD-E2d means 3-story single-diagonal BRBFs with e of 2 times beam depth.

Design Considerations and Results

Brace Design

The overall frame design results are summarized in Table 1. For brace design, three-dimensional frame models representing the example buildings with various design cases of BRBFs were developed in the structural analysis software ETABS (CSI, 2019). Each ETABS model was analyzed for both equivalent lateral force (ELF) and the modal response spectrum analysis (MRSA) to estimate the brace design

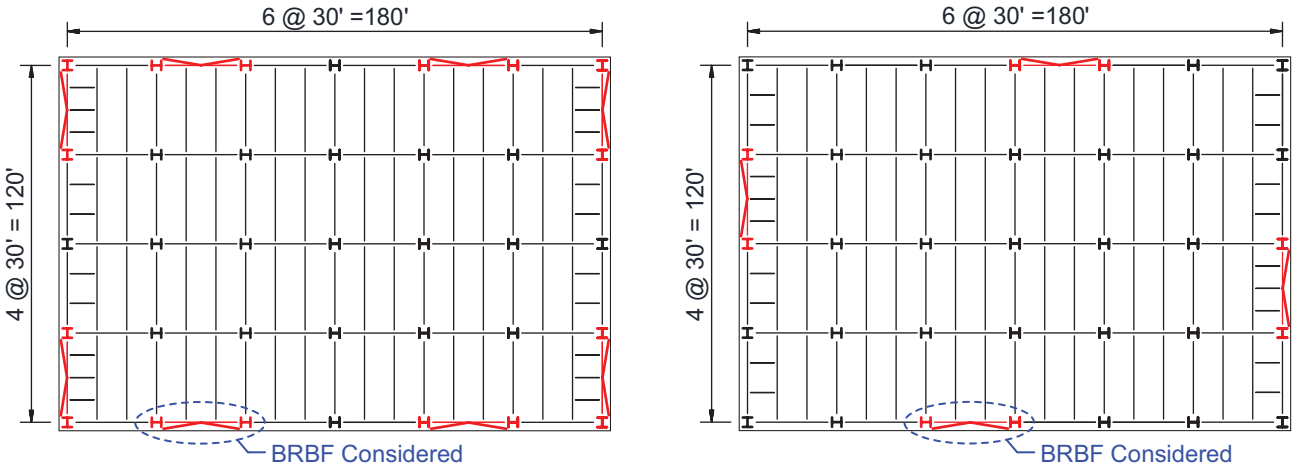

(a) 12-story design cases (b) 3-story design cases

Fig. 14. Floor plans for case study designs.

forces and story drifts. For most of the design cases considered in this study, the MRSA led to a more economical brace design than the ELF method did. Thus, the brace sizes determined from the MRSA are employed for all the design cases with an attempt to pursue the most economical code-permitted BRBF design.

The brace core areas, A_{sc}, rounded up to the nearest 0.5 in.^{2} precision, were sized based on the minimum yield stress of steel core, $F_{ysc,\min}$, of 38 ksi and a strength reduction factor $\phi = 0.9$. Tables 2 and 3 summarize the brace design results alongside the axial demand-to-capacity ratios (DCRs). The DCR for axial force is given by $DCR_P = P_u/(\phi A_{sc} F_{ysc,\min})$. These values are based on the brace force demand, P_u, estimated from the MRSA. The table also presents the design earthquake (DE) story-drift ratios (SDRs), SDR_{DE}, which were determined by amplifying the story drift ratios obtained from MRSA by a factor of (C_d/I_e). As shown in both Tables 2 and 3, all the DCR_P values are less than 1 and most of them are higher than 0.85, indicating an economical design of the braces. All the

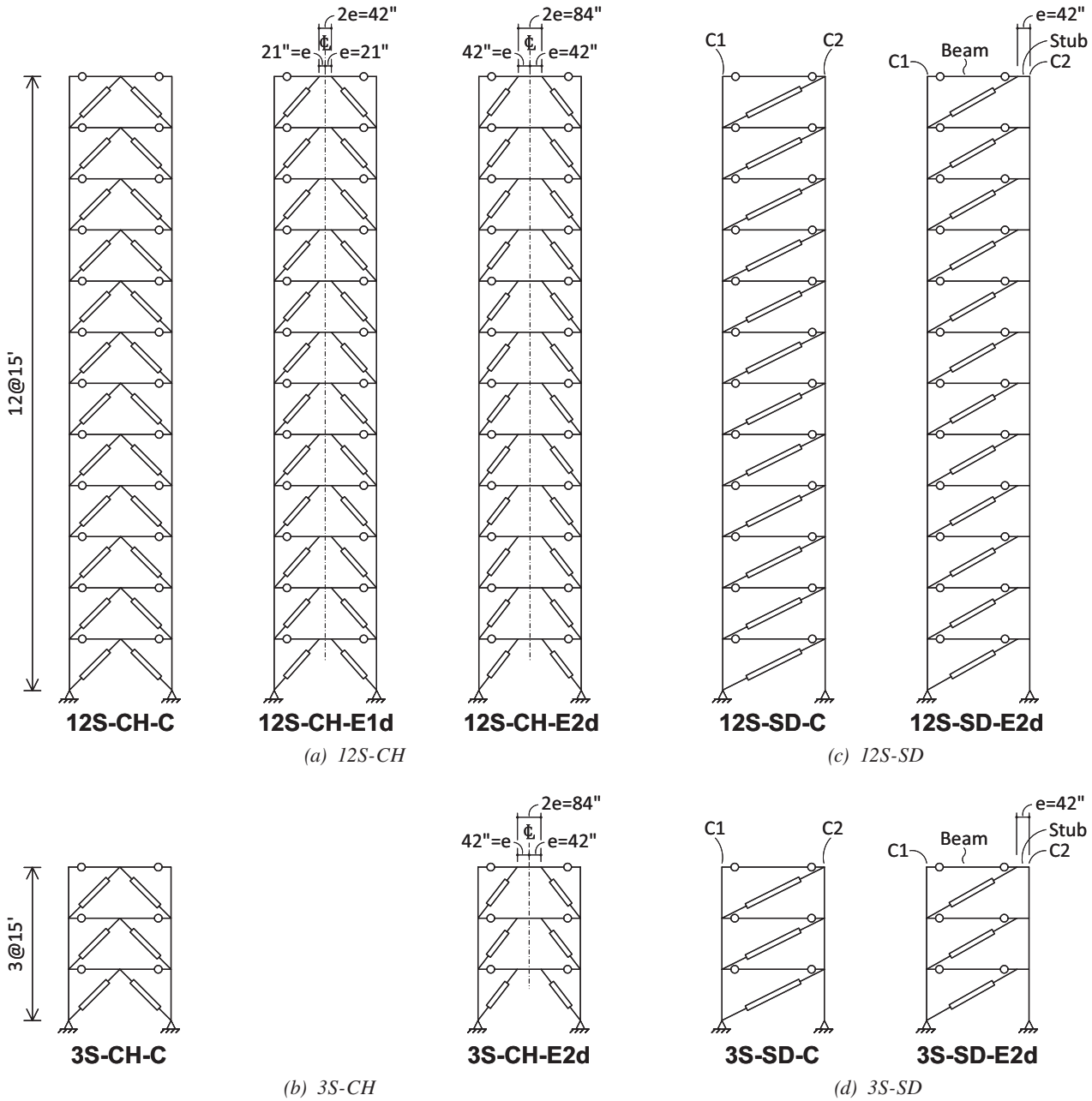

(a) 12S-CH

(c) 12S-SD

(b) 3S-CH

(d) 3S-SD

Fig. 15. Elevations for BRBF designs.

Table 1. Member Sizes for 3- and 12-Story Frames

Member	3-Story (3S) BRBF Design Cases				Member	12-Story (12S) Design Cases				
	CH-C	CH-E2d	SD-C	SD-E2d		CH-C	CH-E1d	CH-E2d	SD-C	SD-E2d
BRB3	3.0	3.5	4.5	3.5	BRB12	1.5	1.5	2.0	2.5	2.0
BRB2	5.0	6.0	8.0	7.0	BRB11	2.5	2.5	3.0	4.0	3.5
BRB1	6.0	7.0	10.0	9.0	BRB10	2.5	3.0	3.5	4.5	4.0
Bm3	W21×44	W21×68	W21×44	W21×44	BRB9	3.0	3.5	4.0	5.0	4.5
Bm1-Bm2	W21×57	W21×132	W21×83	W21×68	BRB8	3.0	3.5	4.0	5.5	5.0
Stub3	—*	—*	—*	W21×55	BRB7	3.5	4.0	4.5	6.0	5.5
Stub1-Stub2	—*	—*	—*	W21×111	BRB6	3.5	4.0	4.5	6.5	6.0
RC1-RC3†	W14×68	W14×74	W12×79	W14×109	BRB5	4.0	4.5	5.0	7.0	6.5
LC1-LC3†	—‡	—‡	W14×68	W14×61	BRB4	4.5	4.5	5.0	7.5	7.0
					BRB3	5.0	5.0	5.5	8.0	7.5
					BRB2	5.5	5.5	6.0	8.5	8.0
					BRB1	5.5	6.0	6.5	9.0	8.5
					Bm9-Bm12	W21×44	W21×62	W21×83	W21×55	W21×55
					Bm5-Bm8	W21×44	W21×68	W21×101	W21×68	W21×62
					Bm1-Bm4	W21×50	W21×83	W21×122	W21×73	W21×68
					Stub9-Stub12	—*	—*	—*	—*	W21×68
					Stub5-Stub8	—*	—*	—*	—*	W21×93
					Stub1-Stub4	—*	—*	—*	—*	W21×111
					RC11-RC12†	W14×43	W14×38	W14×34	W14×43	W14×48
					RC9-RC10†	W14×68	W14×68	W14×68	W14×82	W14×82
					RC7-RC8†	W14×109	W14×109	W14×109	W14×109	W14×120
					RC5-RC6†	W14×132	W14×132	W14×145	W14×145	W14×159
					RC3-RC4†	W14×176	W14×176	W14×193	W14×193	W14×211
					RC1-RC2†	W14×233	W14×233	W14×233	W14×257	W14×257
					LC1-LC12†	—‡	—‡	—‡	—§	W14×38
					LC9-LC10†	—‡	—‡	—‡	—§	W14×68
					LC7-LC8†	—‡	—‡	—‡	—§	W14×109
					LC5-LC6†	—‡	—‡	—‡	—§	W14×145
					LC3-LC4†	—‡	—‡	—‡	—§	W14×193
					LC1-LC2†	—‡	—‡	—‡	—§	W14×257

* Stubs are not used

† In single-diagonal BRBFs, the left column (LC) and right column (RC) represent Column 1 (C1) and Column 2 (C2), respectively.

‡ The same shape is used for RC and LC as the force demands in both sides of columns are identical in chevron BRBFs.

§ The demands in LC (C1) and RC (C2) are different, but the same shape is used for both sides as the demand difference is not large.

SDR_{DE} ratios are lower than the code-allowable limit of 2%, and most of them are less than 2% by a considerable margin, reflecting the fact that the brace design is governed by strength for majority of the braces in these design cases.

From the variations in A_{sc} and SDR_{DE} values among the design cases in each chevron BRBF Group [Groups 12S-CH (Table 2) or 3S-CH (Table 3)], it can be found that, in the chevron BRBFs, both brace sizes and story drifts increase with the eccentricity. As the eccentricity increases, the brace inclination angle gets steeper, which makes the braces less efficient in providing the lateral stiffness and resistance to the frame. It is noted that the design of the braces in the top three stories of Design 12S-CH-E2d is governed by story-drift check rather than strength design.

Table 2. BRB Axial DCRs (DCR_P) and Design Story-Drift Ratios (SDR_{DE}) for 12-Story BRBFs

Story	Group 12S-CH (12-Story Chevron BRBFs)								
	12S-CH-C			12S-CH-E1d			12S-CH-E2d		
	BRB		SDR_{DE}	BRB		SDR_{DE}	BRB		SDR_{DE}
	A_{sc} (in.^{2})	DCR_P	(%)	A_{sc} (in.^{2})	DCR_P	(%)	A_{sc} (in.^{2})	DCR_P	(%)
12	1.5	0.84	1.53	1.5	0.92	1.64	2.0*	0.75	1.67
11	2.5	0.83	1.63	2.5	0.89	1.78	3.0*	0.81	1.85
10	2.5	0.98	1.73	3.0	0.89	1.81	3.5*	0.84	1.93
9	3.0	0.91	1.62	3.5	0.86	1.74	4.0	0.83	1.88
8	3.0	0.95	1.58	3.5	0.91	1.70	4.0	0.91	1.82
7	3.5	0.91	1.44	4.0	0.89	1.56	4.5	0.89	1.74
6	3.5	0.95	1.35	4.0	0.94	1.48	4.5	0.94	1.70
5	4.0	0.94	1.17	4.5	0.92	1.36	5.0	0.92	1.58
4	4.5	0.91	1.04	4.5	0.98	1.25	5.0	0.99	1.46
3	5.0	0.90	0.90	5.0	0.98	1.11	5.5	0.98	1.33
2	5.5	0.91	0.77	5.5	0.96	0.99	6.0	0.97	1.22
1	5.5	0.97	0.71	6.0	0.96	0.87	6.5	0.97	1.12

Story	Group 12S-SD (12-Story Single-Diagonal BRBFs)					
	12S-SD-C			12S-SD-E2d		
	BRB		SDR_{DE}	BRB		SDR_{DE}
	A_{sc} (in.^{2})	DCR_P	(%)	A_{sc} (in.^{2})	DCR_P	(%)
12	2.5	0.82	1.85	2.0	0.85	1.84
11	4.0	0.83	1.87	3.5	0.86	1.89
10	4.5	0.88	1.92	4.0	0.88	1.85
9	5.0	0.87	1.87	4.5	0.87	1.80
8	5.5	0.86	1.77	5.0	0.85	1.68
7	6.0	0.85	1.64	5.5	0.84	1.56
6	6.5	0.85	1.52	6.0	0.83	1.42
5	7.0	0.85	1.39	6.5	0.83	1.30
4	7.5	0.87	1.26	7.0	0.84	1.17
3	8.0	0.90	1.14	7.5	0.86	1.06
2	8.5	0.93	1.03	8.0	0.89	0.94
1	9.0	0.93	0.98	8.5	0.95	0.94

* Sizing of BRBs is governed by story drift check: $SDR_{DE} \leq 2\%$

On the other hand, the tabulated A_{sc} and SDR_{DE} values in the single-diagonal BRBF groups [i.e., Groups 12S-SD (Table 2) and 3S-SD (Table 3)] show that both brace sizes and story drifts generally get reduced when the eccentricity is introduced in the single-diagonal BRBFs. This is attributed to the fact that the moment connections between the stubs and Column 2 (C2) members make the C2 members resist moments as well as shears under the seismic loading. Hence, in the single-diagonal eccentric BRBFs, the C2 members participate in providing the lateral-force-resisting stiffness and strength, leading to less force demands in the braces. Further, the design cases in this study show that, for the single-diagonal BRBFs, the BRBF with eccentricity tend to have higher lateral stiffness than the concentric BRBF.

Table 3. BRB Axial DCRs (DCR_P) and Design Story-Drift Ratios (SDR_{DE}) for 3-Story BRBFs												
Story	Group 3S-CH (3-Story Chevron BRBFs)						Group 3S-SD (3-Story Single-Diagonal BRBFs)					
	3S-CH-C			3S-CH-E2d			3S-SD-C			3S-SD-E2d		
	BRB		SDR_{DE}	BRB		SDR_{DE}	BRB		SDR_{DE}	BRB		SDR_{DE}
	A_{sc} (in.^{2})	DCR_P	(%)	A_{sc} (in.^{2})	DCR_P	(%)	A_{sc} (in.^{2})	DCR_P	(%)	A_{sc} (in.^{2})	DCR_P	(%)
3	3.0	0.89	0.92	3.5	0.88	1.06	4.5	0.92	1.07	3.5	0.95	1.02
2	5.0	0.93	0.88	6.0	0.94	1.00	8.0	0.92	1.00	7.0	0.93	0.92
1	6.0	0.98	0.77	7.0	0.97	0.97	10.0	0.92	0.94	9.0	0.97	1.02

Table 4. BRB Properties for 12-Story Chevron BRBFs																		
Story	12S-CH-C						12S-CH-E1d						12S-CH-E2d					
	A_{sc} (in.^{2})	L_{ysc} (in.)	ε_{BRB} (in./in.)	KF	ω	ωβ	A_{sc} (in.^{2})	L_{ysc} (in.)	ε_{BRB} (in./in.)	KF	ω	ωβ	A_{sc} (in.^{2})	L_{ysc} (in.)	ε_{BRB} (in./in.)	KF	ω	ωβ
12	1.5	130	0.0197	1.58	1.37	1.59	1.5	119	0.0202	1.61	1.38	1.60	2.0	148	0.0150	1.38	1.29	1.44
11	2.5	171	0.0150	1.33	1.29	1.44	2.5	159	0.0151	1.35	1.30	1.46	3.0	146	0.0151	1.36	1.30	1.46
10	2.5	171	0.0150	1.33	1.29	1.44	3.0	157	0.0152	1.35	1.30	1.46	3.5	144	0.0153	1.37	1.30	1.46
9	3.0	170	0.0151	1.33	1.30	1.46	3.5	156	0.0154	1.35	1.30	1.47	4.0	137	0.0162	1.44	1.32	1.49
8	3.0	170	0.0151	1.33	1.30	1.46	3.5	156	0.0154	1.35	1.30	1.47	4.0	137	0.0162	1.44	1.32	1.49
7	3.5	168	0.0152	1.34	1.30	1.46	4.0	148	0.0162	1.42	1.32	1.49	4.5	138	0.0160	1.41	1.31	1.48
6	3.5	168	0.0152	1.34	1.30	1.46	4.0	148	0.0162	1.42	1.32	1.49	4.5	138	0.0160	1.41	1.31	1.48
5	4.0	161	0.0159	1.40	1.31	1.48	4.5	150	0.0160	1.38	1.31	1.48	5.0	137	0.0161	1.42	1.31	1.48
4	4.5	163	0.0157	1.37	1.31	1.48	4.5	150	0.0160	1.39	1.31	1.48	5.0	137	0.0161	1.42	1.31	1.48
3	5.0	162	0.0157	1.37	1.31	1.48	5.0	149	0.0161	1.40	1.31	1.48	5.5	134	0.0165	1.46	1.32	1.49
2	5.5	159	0.0160	1.40	1.31	1.48	5.5	146	0.0163	1.43	1.32	1.49	6.0	129	0.0171	1.49	1.33	1.52
1	5.5	163	0.0157	1.38	1.31	1.48	6.0	143	0.0167	1.45	1.33	1.50	6.5	128	0.0172	1.50	1.33	1.52

Table 5. BRB Properties for 12-Story Single-Diagonal BRBFs												
Story	12S-SD-C						12S-SD-E2d					
	A_{sc} (in.^{2})	L_{ysc} (in.)	ε_{BRB} (in./in.)	KF	ω	ωβ	A_{sc} (in.^{2})	L_{ysc} (in.)	ε_{BRB} (in./in.)	KF	ω	ωβ
12	2.5	291	0.0111	1.28	1.23	1.35	2.0	260	0.0121	1.30	1.23	1.35
11	4.0	281	0.0115	1.32	1.23	1.35	3.5	257	0.0122	1.29	1.24	1.36
10	4.5	282	0.0114	1.29	1.23	1.35	4.0	250	0.0126	1.34	1.25	1.39
9	5.0	282	0.0114	1.30	1.23	1.35	4.5	251	0.0125	1.31	1.24	1.38
8	5.5	279	0.0116	1.32	1.23	1.35	5.0	250	0.0125	1.32	1.24	1.38
7	6.0	274	0.0118	1.34	1.23	1.35	5.5	247	0.0127	1.34	1.25	1.39
6	6.5	273	0.0118	1.34	1.23	1.35	6.0	243	0.0129	1.36	1.25	1.39
5	7.0	271	0.0119	1.34	1.23	1.35	6.5	242	0.0130	1.36	1.25	1.39
4	7.5	270	0.0119	1.34	1.23	1.35	7.0	240	0.0131	1.36	1.26	1.40
3	8.0	263	0.0123	1.37	1.24	1.36	7.5	239	0.0131	1.36	1.26	1.40
2	8.5	262	0.0123	1.37	1.24	1.36	8.0	232	0.0135	1.39	1.27	1.41
1	9.0	283	0.0114	1.29	1.23	1.35	8.5	249	0.0126	1.31	1.25	1.39

Table 6. BRB Properties for 3-Story Chevron BRBFs												
Story	3S-CH-C						3S-CH-E2d					
	A_{sc} (in.^{2})	L_{ysc} (in.)	ε_{BRB} (in./in.)	KF	ω	ωβ	A_{sc} (in.^{2})	L_{ysc} (in.)	ε_{BRB} (in./in.)	KF	ω	ωβ
3	3.0	169	0.0151	1.34	1.30	1.46	3.5	144	0.0153	1.37	1.30	1.46
2	5.0	161	0.0159	1.38	1.31	1.48	6.0	131	0.0169	1.48	1.33	1.52
1	6.0	159	0.0160	1.40	1.31	1.48	7.0	125	0.0177	1.50	1.34	1.53

Table 7. BRB Properties for 3-Story Single-Diagonal BRBFs												
Story	3S-SD-C						3S-SD-E2d					
	A_{sc} (in.^{2})	L_{ysc} (in.)	ε_{BRB} (in./in.)	KF	ω	ωβ	A_{sc} (in.^{2})	L_{ysc} (in.)	ε_{BRB} (in./in.)	KF	ω	ωβ
3	4.5	282	0.0114	1.30	1.23	1.35	3.5	258	0.0121	1.29	1.24	1.36
2	8.0	262	0.0123	1.37	1.24	1.36	7.0	241	0.0130	1.35	1.25	1.39
1	10.0	279	0.0116	1.31	1.23	1.35	9.0	250	0.0125	1.31	1.24	1.38

Capacity Design

The BRB design parameters, including the stiffness modification factor (KF) and strength adjustment factors, ω and β, are listed in Tables 4 through 7. These tabulated ω and β values are based on the tabulated core strain, ε_{BRB}, which is corresponding to an assumed 2% controlling story drift, the minimum allowed by the AISC *Seismic Provisions* (2016a) for calculating the expected BRB deformations. The BRBF beams and columns were assumed to be ASTM A992 (2022) steel W-shape members and sized for the capacity design considering the adjusted brace strengths in tension and compression, P_{uT} and P_{uC}. These strengths were computed using Equations 1 and 2, with the maximum yield stress, $F_{ysc,\max}$ = 46 ksi as an estimate of the actual yield stress of steel core, F_{ysc}, and the values of ω and β factors tabulated in Tables 4 through 7. Detailed descriptions of capacity designs for beams and columns follow.

Beam Design

Beam sizing in this study is based on two main criteria: capacity design and sectional compactness satisfying moderately ductile requirements, with the former governing all the cases. As shown in Figures 6, 9, and 10, the capacity design of BRBF beams considers the force demands from the superposition of gravity and capacity-limited seismic effects. For BRBFs with eccentricities, the beam at each floor is divided into multiple regions or members by the brace-to-beam intersection points, such as the three beam regions in the chevron bracing case and the stub and beam members in the single-diagonal bracing case. Each beam region or member must be checked to remain essentially elastic for both *P-M* and *P-V* interaction demands.

The DCR for the *P-M* interaction, DCR_{PM}, is calculated in accordance with AISC *Specification* Chapter H (2016b) as follows:

$$DCR_{PM} = \begin{cases} \left|\frac{P_u}{\phi P_n}\right| + \frac{8}{9}\left|\frac{M_u}{\phi_b M_n}\right|, \ for \left|\frac{P_u}{\phi P_n}\right| \geq 0.2 \\ \frac{1}{2}\left|\frac{P_u}{\phi P_n}\right| + \left|\frac{M_u}{\phi_b M_n}\right|, \ for \left|\frac{P_u}{\phi P_n}\right| < 0.2 \end{cases} \quad (28)$$

where the design axial strength, ϕP_n, is taken as the tensile yielding strength, $\phi_t P_y$, if the axial demand, P_u, is in tension, while the compressive strength $\phi_c P_n$ is used when P_u is compressive. Also, $\phi_b M_n$ is the design flexural strength. Note that for the BRBF beams, the compressive strength, $\phi_c P_n$, was determined considering several possible buckling modes, including strong-axis flexural buckling, torsional buckling, and constrained-axis torsional buckling (Timoshenko and Gere, 1961).

To quantify the DCR for the *P-V* interaction in the BRBF beams, DCR_{PV}, the formula for determining the shear strength of the shear-yielding links in the EBF stipulated in the AISC *Seismic Provisions* is adopted herein. DCR_{PV} is computed from:

$$DCR_{PV} = \frac{V_u}{\phi_v V_p^*} \quad (29)$$

where ϕ_v = 0.9 and V_p^* is the reduced plastic shear strength of W-shape member considering the presence of axial force demand P_u. The equation for V_p^* is as follows:

Table 8. Beam Design DCRs for 12-Story BRBFs									
Level	Group 12S-CH (12-Story Chevron BRBFs)								
	12S-CH-C			12S-CH-E1d			12S-CH-E2d		
	Beam			Beam			Beam		
	Shape	DCR		Shape	DCR		Shape	DCR	
		P-M	*Chev**		*P-M*	*P-V*		*P-M*	*P-V*
12	W21×44	0.51	0.33	W21×62	0.46	0.32	W21×83	0.56	0.28
11		0.85	0.51		0.73	0.49		0.83	0.43
10		0.85	0.51		0.82	0.59		0.91	0.50
9		0.85	0.62		0.87	0.69		0.99	0.58
8	W21×44	0.85	0.62	W21×68	0.78	0.65	W21×101	0.76	0.59
7		0.85	0.72		0.85	0.75		0.82	0.66
6		0.85	0.72		0.85	0.75		0.82	0.66
5		0.85	0.76		0.90	0.84		0.88	0.73
4	W21×50	0.74	0.78	W21×83	0.73	0.70	W21×122	0.72	0.61
3		0.74	0.87		0.78	0.78		0.78	0.68
2		0.80	0.96		0.83	0.86		0.87	0.75
1		0.80	0.95		0.88	0.95		0.96	0.81
Level	Group 12S-SD (12-Story Single-Diagonal BRBFs)								
	12S-SD-C			12S-SD-E2d					
	Beam			Beam			Stub		
	Shape	DCR		Shape	DCR		Shape	DCR	
		P-M	*P-V*		*P-M*	*P-V*		*P-M*	*P-V*
12	W21×55	0.43	0.09	W21×55	0.37	0.10	W21×68	0.47	0.33
11		0.82	0.13		0.69	0.15		0.76	0.56
10		0.94	0.14		0.80	0.15		0.84	0.62
9		0.99	0.14		0.85	0.15		0.91	0.68
8	W21×68	0.80	0.12	W21×62	0.77	0.14	W21×93	0.72	0.55
7		0.84	0.12		0.82	0.14		0.79	0.60
6		0.88	0.12		0.87	0.14		0.85	0.65
5		0.92	0.12		0.91	0.14		0.91	0.69
4	W21×73	0.88	0.12	W21×68	0.85	0.13	W21×111	0.77	0.78
3		0.92	0.12		0.90	0.13		0.82	0.83
2		0.96	0.12		0.94	0.14		0.87	0.89
1		1.00	0.12		0.98	0.14		0.91	0.92
* Design for chevron effect (Sabelli and Arber, 2017)									

$$V_p^* = \begin{cases} 0.6F_yA_{lw} & , for \left|\frac{P_u}{P_y}\right| \le 0.15 \\ 0.6F_yA_{lw}\sqrt{1-(P_u/P_y)^2} & , for \left|\frac{P_u}{P_y}\right| > 0.15 \end{cases} \quad (30)$$

where $A_{lw} = (d - 2t_f)t_w$ estimates the shear area of beam web considering the clear distance between the flanges and $P_y = F_yA_g$ is the nominal axial yielding strength of the gross beam section.

Tables 8 and 9 summarize the beam design results, including the selected W-shapes and the calculated DCRs (DCR_{PM} and DCR_{PV}) for all design cases. For the 12-story design cases (Table 8), identical beam sections were

Table 9. Beam Design DCRs for 3-Story BRBFs															
Level	Group 3S-CH (3-Story Chevron BRBFs)						Group 3S-SD (3-Story Single-Diagonal BRBFs)								
	3S-CH-C			3S-CH-E2d			3S-SD-C			3S-SD-E2d					
	Beam			Beam			Beam			Beam			Stub		
	Shape	DCR		Shape	DCR		Shape	DCR		Shape	DCR		Shape	DCR	
		P-M	*Chev**		*P-M*	*P-V*		*P-M*	*P-V*		*P-M*	*P-V*		*P-M*	*P-V*
3	W21×44	0.57	0.62	W21×68	0.99	0.59	W21×44	0.81	0.10	W21×44	0.65	0.11	W21×55	0.94	0.60
2	W21×57	0.63	0.73	W21×132	0.80	0.69	W21×83	0.71	0.10	W21×68	0.73	0.13	W21×111	0.79	0.78
1	W21×57	0.75	0.83	W21×132	0.97	0.81	W21×83	0.89	0.10	W21×68	0.95	0.14	W21×111	0.96	0.96
* Design for chevron effect (Sabelli and Arber, 2017)															

selected for every four floors. For 3-story cases (Table 9), different beam sections were used between the roof level and the other two floors. For the beams in chevron eccentric BRBFs, the governing (i.e., maximum) DCR_{PV} values occur in the interior segment, while the governing DCR_{PM} values come from the exterior segments. For the chevron BRBFs with eccentricity at one beam depth (CH-E1d cases), DCR_{PV} is higher than DCR_{PM} only in the bottom two stories of 12S-CH-E1d and in the first story of 3S-CH-E1d, whereas DCR_{PM} is greater than DCR_{PV} in all remaining stories of the two frames. When the eccentricity increases to twice beam depth (CH-E2d cases), DCR_{PM} is higher than DCR_{PV} over the entire building height in both 12S-CH-E2d and 3S-CH-E2d. It seems to suggest that, in multistory eccentrically chevron BRBFs, the design of the beams at intermediate through upper floors tend to be governed by the *P-M* interaction, whereas the beam design may be governed the *P-V* interaction at lower floors, where the brace forces acting on the beams are higher. Further, as the eccentricity increases, the beam design would lean more toward being governed by the *P-M* interaction.

For the concentrically chevron BRBFs (12S-CH-C and 3S-CH-C), the shear strength check for the beams was based on the design method proposed by Sabelli and Arber (2017) that considers the chevron effect, inducing the localized force demands in a beam within the in-span gusset plate region. The associated DCR, DCR_{Chev}, is defined as the ratio of the minimum required gusset plate length to the actual gusset plate length provided. A value of DCR_{Chev} less than 1.0 means that the original section of a beam is strong enough to handle the local force demand with no need for strengthening the beam web with doubler plates. For Case 12S-CH-C (see Table 8), the beam design is governed by the chevron effect, as evidenced by the fact $DCR_{Chev} > DCR_{PM}$, in the bottom four levels, while the design of remaining beams is governed by *P-M* interaction. In 3S-CH-C (Table 9), the chevron effect governs the design for all the beams. Moreover, by comparing the beam sizes among the design cases in each chevron BRBF group [Groups 12S-CH (Table 8) or 3S-CH (Table 9)], it is apparent that the beam sizes are increased with the bracing eccentricity in the chevron BRBFs.

For both concentrical and eccentric single-diagonal BRBFs, it is apparent from Tables 8 and 9 that DCR_{PM} values are much higher than DCR_{PV} values for the beam members, indicating that the design of these pinned-end beam members is governed by the *P-M* interaction, where the moment demand is due to the gravity effects only. By comparing the concentric and eccentric cases, it can be seen that the sizes of the pinned beam members could be slightly reduced as the bracing eccentricity is introduced to single-diagonal BRBFs. This is primarily due to the shorter beam lengths and smaller horizontal brace forces (due to the smaller braces and steeper brace angle) in the eccentric bracing configuration. In the single-diagonal BRBFs with eccentricity [12S-SD-E2d (Table 8) and 3S-SD-E2d (Table 9)], the sizes of the stubs are notably larger than the pinned beams because of the high seismic shear and moment demands in the stubs. The stub design is governed by *P-V* interaction for the bottom floors in 12S-SD-E2d, while *P-M* interaction governs the design for the stubs at the remaining floors. Although the design of all the stubs in 3S-SD-E2d is governed by *P-M* interaction, the DCR values for the *P-V* interaction are also very high for stubs at the bottom two floors. These seem to suggest that the stub design in the lower floors have a higher chance to be governed by the *P-V* interaction.

Column Design

The column sizing is based on capacity design and compactness requirements for moderately ductile members. As permitted by the AISC *Seismic Provisions* (2016a), the capacity design of BRBF columns for the all design cases presented in this Part 1 paper considered the axial force demand (P_u) only, where P_u was calculated by superimposing gravity effects with capacity-limited seismic effects (as illustrated in Figures 11–13), assuming all braces simultaneously develop their adjusted strength in compression or

Table 10. Column Compressive Axial DCR (DCR_P) for 12-Story BRBFs

Story	12S-CH-C		12S-CH-E1d		12S-CH-E2d		12S-SD-C				12S-SD-E2d			
	Column		Column		Column		Column 1 (C1)		Column 2 (C2)		Column 1 (C1)		Column 2 (C2)	
	Shape	DCR_P	Shape	DCR_P	Shape	DCR_P	Shape	DCR_P	Shape	DCR_P	Shape	DCR_P	Shape	DCR_P
12	W14×43	0.16	W14×38	0.20	W14×34	0.14	W14×43	0.18	W14×43	0.39	W14×38	0.26	W14×48	0.33
11	W14×43	0.66	W14×38	0.92	W14×34	0.97	W14×43	0.67	W14×43	0.99	W14×38	0.97	W14××48	0.86
10	W14×68	0.62	W14×68	0.57	W14×68	0.56	W14×82	0.52	W14×82	0.65	W14×68	0.59	W14×82	0.65
9	W14×68	0.92	W14×68	0.89	W14×68	0.89	W14×82	0.79	W14×82	0.92	W14×68	0.92	W14×82	0.93
8	W14×109*	0.63	W14×109*	0.63	W14×109*	0.64	W14×109*	0.65	W14×109	0.73	W14×109*	0.63	W14×120	0.67
7	W14×109*	0.80	W14×109*	0.81	W14×109*	0.82	W14×109*	0.84	W14×109	0.92	W14×109*	0.82	W14×120	0.84
6	W14×132	0.82	W14×132	0.83	W14×145	0.75	W14××145	0.76	W14×145	0.82	W14×145	0.75	W14×159	0.76
5	W14×132	0.97	W14×132	1.00	W14×145	0.90	W14×145	0.92	W14×145	0.97	W14×145	0.91	W14×159	0.91
4	W14×176	0.84	W14×176	0.86	W14×193	0.80	W14×193	0.81	W14×193	0.85	W14×193	0.80	W14×211	0.79
3	W14×176	0.98	W14×176	0.99	W14×193	0.91	W14×193	0.94	W14×193	0.97	W14×193	0.93	W14×211	0.91
2	W14×233	0.85	W14×233	0.85	W14×233	0.86	W14×257	0.80	W14×257	0.82	W14×257	0.80	W14×257	0.85
1	W14×233	0.97	W14×233	0.96	W14×233	0.97	W14×257	0.91	W14×257	0.93	W14×257	0.91	W14×257	0.96

* Column design is governed by sectional compactness requirement of moderately ductile members

Table 11. Column Compressive Axial DCR (DCR_P) for 3-Story BRBFs

Story	3S-CH-C		3S-CH-E2d		3S-SD-C				3S-SD-E2d			
	Column		Column		Column 1 (C1)		Column 2 (C2)		Column 1 (C1)		Column 2 (C2)	
	Shape	DCR_P	Shape	DCR_P	Shape	DCR_P	Shape	DCR_P	Shape	DCR_P	Shape	DCR_P
12	W14×68	0.07	W14×74	0.06	W14×68	0.08	W12×79	0.20	W14×61	0.09	W14×109*	0.13
11	W14×68	0.40	W14×74	0.42	W14×68	0.41	W12×79	0.55	W14×61	0.42	W14×109*	0.35
10	W14×68	0.90	W14×74	0.99	W14×68	0.90	W12×79	0.95	W14×61	0.96	W14×109*	0.62

* Column design is governed by sectional compactness requirement of moderately ductile members

tension. Moderately ductile member requirements, rather than highly ductile ones, were applied to the columns in the case study BRBFs to achieve a more efficient design and enable clearer observation of eccentricity effects on column sizes. This approach followed design requirements outlined in the 2016 AISC *Seismic Provisions* (2016a), which required columns to only be moderately ductile. Tables 10 and 11 summarize the column design results alongside the values of axial DCRs, $DCR_P = P_u/(\phi_c P_n)$, where $\phi_c P_n$ is the design compressive strength. W14 sections were chosen to be the default size for all columns. For the 12-story cases, identical column sizes were selected for every two stories. For the 3-story cases, the same column sizes were used for all three stories. The asterisk (*) in these two tables marks the columns that were sized based on the compactness requirement instead of capacity design.

In the chevron BRBF cases, it appears that column sizes increase with eccentricity in a "slow" manner. In comparing 12S-CH-C and 12S-CH-E1d (Table 10), all the columns except for the top two stories are the same. Comparing 12S-CH-E1d and -E2d, the column sizes are heavier only in some levels (the 3rd to 6th stories) of 12S-CH-E2d. Also, as shown in Table 11, the column size in 3S-CH-E2d is slightly heavier than that in 3S-CH-C. It has been shown in Tables 2, 3, 8, and 9 that a notable increase in both brace and beam sizes with the bracing eccentricity is observed in all levels of chevron BRBFs. By contrast, the rate of increase in column sizes with the bracing eccentricity is much slower. This is attributed to the fact that the beam-end shears and the vertical brace forces delivered to the columns are acting in the opposite direction [Equation 11(b)] in the chevron BRBFs. Although the column axial force demands are generally increased with the bracing eccentricity because of

the increased vertical brace force, the increased beam end shears essentially offset the increase in the column axial force demand with the eccentricity.

For single-diagonal BRBF cases, the two sides of columns (i.e., C1 and C2 members, to which the bottom and top ends of braces are adjacent, respectively) in each frame were designed separately. In any story, the C2 member is designed for higher capacity-limited axial forces than the C1 member in the same story because the C2 member resists the vertical forces from one more brace than the C1 member does. The discrepancy of axial demand between two sides of column is notable for low-rise BRBFs but may become insignificant for high-rise BRBFs, especially on the columns in the lower stories. Take, for example, the concentric design cases: The design of 3S-SD-C (Table 11) ended up with different column sizes between C1 and C2 members, while the same column sizes were selected for the two sides of 12S-SD-C (Table 10). It can be found that in 12S-SD-C, the DCR_P values of C1 members are smaller than those of C2 members over the entire building height, and discrepancy in DCR_P between the two sides of columns is diminishing as it goes from top to bottom of the building. The low DCR_P values for the C1 members in the top part (9th to 12th stories) of 12S-SD-C indicates a potential for using lighter columns. However, no commercially available lighter sections can be selected for these columns.

For the single-diagonal eccentric BRBF design cases, the discrepancy in the axial force demand between C1 and C2 members becomes more significant than that in the concentric design cases because the moment connections used between the stubs and C2 members is much stiffer than the pin connections between the beam and C1 members, causing C2 members to carry more gravity loads than C1 members. Therefore, for both 12S-SD-E2d (Table 10) and 3SD-SD-E2d (Table 11), except for the bottom two stories of 12-SD-E2d, the C2 members are heavier than C1 members over the building height.

Moreover, by comparing the column sizes between the concentric (-C) and eccentric (-E2d) cases in each single-diagonal BRBF group [Groups 12S-SD (Table 10) or 3S-SD (Table 11)], it can be seen that eccentricity can make C1 members lighter while C2 members get heavier. This would be mainly attributed to the fact that uneven gravity loads are distributed to the C1 and C2 members in the eccentric cases. Another factor varying the column axial demands with the eccentricity is the change of the vertical component of brace forces delivered to the columns, which is related to the changes in size and inclination angle for the braces. However, this factor is shown to be insignificant from the design cases in this study. Although the brace sizes as well as the brace adjusted strengths become smaller when the eccentricity increases, the steeper brace angle would lead to greater vertical components of the brace forces. These two effects are counteractive, making the resulting vertical components of brace forces delivered to the columns similar, regardless of eccentricity.

Weight Comparison

Tables 12 and 13 respectively, present the steel weights for the 12-story and 3-story case study designs. For the group of chevron BRBF design cases, the brace steel weights (including casing but excluding the infill grout) were similar among the three 12-story design cases (12S-CH-C, 12S-CH-E1d, and 12S-CH-E2d). Likewise, the brace steel weights of the two 3-story chevron cases (3S-CH-C and 3S-CH-E2d) were close. These results indicate that the increase in core area with eccentricity was offset by the shorter brace lengths and casing weight. Furthermore, in each chevron group (Groups 12S-CH or 3S-CH), the column weights were similar between the cases, reflecting that the column sizes slowly increase with the eccentricity for chevron BRBFs. However, for both Groups 12S-CH and 3S-CH, the beams were substantially heavier for the BRBFs with eccentricities. Case 12S-CH-E2d is more than double the beam weight as compared to the concentric case (12S-CH-C). Similarly, the beam weight in Case 3S-CH-E2d is about twice that in 3S-CH-C. Overall, it is apparent that the total steel weight increases with the eccentricity for the chevron BRBFs. For Group 12S-CH, Case 12S-CH-E1d was 1.10 times heavier than the concentric Case 12S-CH-C, and 12S-CH-E2d was 1.27 times heavier. For Group 3S-CH, Case 3S-CH-E2d was 1.32 times heavier than the concentric Case 3S-CH-C.

For the single-diagonal BRBF design cases, the brace steel weight in the frames with eccentricities were notably less than their benchmark concentric frames. The brace steel weight in eccentric Case 12S-SD-E2d was about 18% lighter than that in the concentric Case 12S-SD-C. Likewise, the brace steel weight in 3S-SD-E2d was about 24% lighter than that in 3S-SD-C. This is attributed to the fact that C2 members in the eccentric BRBF take partial story shears so that the braces in the eccentric case carry less story shears than those in the concentric case, resulting in the decrease in the steel core area in the eccentric BRBFs. In addition, the brace length was shortened in the eccentric case because of the steeper brace angle. The reduction in brace length and core area results in the notable decrease in the brace steel weight with the eccentricity in the single-diagonal BRBFs. For the column weight, the eccentric Case 12S-SD-E2d was slightly higher than the concentric Case 12S-SD-C. Similarly, for Group 3S-SD, the column weight in Case 3S-SD-E2d was moderately heavier than that in 3S-SD-C. These suggest that, as the eccentricity is introduced into a single-diagonal BRBF, the weight increase in C2 members would be somewhat offset by the weight decrease in the C1 members, resulting in a slight

Table 12. Steel Weights for 12-Story Case Study Designs							
Group	Design	BRB (kips)	Column (kips)	Beam (kips)	Frame (kips)	Frame + BRB (kips)	Increase (%)
12S-CH	12S-CH-C	16.7	45.7	16.6	62.2	78.9	—
	12S-CH-E1d	16.2	45.4	25.6	70.9	87.2	+10.4%
	12S-CH-E2d	16.4	46.9	36.7	83.6	100	+26.8%
12S-SD	12S-SD-C	21.2	49.7	23.5	73.3	94.5	—
	12S-SD-E2d	17.4	50.6	23.4	74.0	91.4	–3.27%
	12S-SD-E2d*	19.3	56.0	24.9	80.9	100	+5.99%

Table 13. Steel Weights for 3-Story Case Study Designs							
Group	Design	BRB (kips)	Column (kips)	Beam (kips)	Frame (kips)	Frame + BRB (kips)	Increase (%)
3S-CH	3S-CH-C	4.83	6.12	4.74	10.9	15.7	—
	3S-CH-E2d	4.74	6.66	9.36	16.0	20.8	+32.3%
3S-SD	3S-SD-C	6.22	6.62	6.30	12.9	19.1	—
	3S-SD-E2d	4.74	7.65	5.74	13.4	18.1	–5.24%
	3S-SD-E2d*	5.32	8.46	6.11	14.6	19.9	+3.91%

increase in the total column weight. For the beam weight, Case 12S-SD-E2d was slightly less than Case 12S-SD-C. Similarly, for Group 3S-SD, the beam weight in 3S-SD-E2d was moderately lighter than that in 3S-SD-C. Compared to the beam sections employed in the concentric frame, lighter sections were used for the beam members (which occupy a large portion of the span width) in the eccentric frame, despite heavier sections required for the short stub members. This results in slightly lighter beam weight in the eccentric frame. Overall, the total weight of Case 12S-SD-E2d was about 3% lighter than 12S-SD-C, while 3S-SD-E2d was about 5% lighter than 3S-SD-C.

Alternative designs were generated neglecting the effects of the half-SMF in resisting story shear. Using this conservative assumption, larger brace sizes were required, and heavier beams and columns were needed to match the capacity of the larger braces. The steel weights for the "re-design" results (denoted as 12S-SD-E2d* and 3S-SD-E2d*) are listed in Tables 12 and 13. The total weight of Case 12S-SD-E2d* was 6% higher than Case 12S-SD-C, while 3S-SD-E2d* was 4% higher than 3S-SD-C. This indicates that neglecting the half-MRF action when designing single-diagonal BRBF with eccentricity would lead to somewhat increased total steel weight

The weight economy for single-diagonal frames in these case study designs is much better than what has been reported in previous studies on BRBFs with eccentricity because of differences in the design approach. In the single-diagonal frames reported by Prinz and Richards (2012), and others that have followed their approach, the stub and beam were selected to be the same size, the columns were designed for the seismic moments, and the beneficial effects of the half-MRF were neglected. Part 2 of this paper (Li et al., 2026) demonstrates that these design assumptions from past studies are overly conservative.

Beam Weight Parameter Study

An additional parameter study was conducted to investigate the beam weight increase when the beam depth is not fixed, as it was for the case-study designs. Allowing the beam depth to increase may result in a more economical beam design. Seven eccentricities (including zero) were investigated in combination with four reference brace areas and two frame configurations (single-diagonal, chevron). The reference brace area established the story shear strength for the concentric case that was matched for all eccentric cases. Beam weights were normalized by the beam weight with zero eccentricity, other things being equal.

Figure 16 shows results from the parameter study. The vertical axis shows total beam weights normalized by the weight of the concentric case. As with the case study designs (Tables 12 and 13), the beam weights increased with eccentricity for the chevron frames. However, for chevron frames with an eccentricity of 48 in., the beam weight increase was less than 2 times, since the beam depth was allowed to vary (Figure 16). For single-diagonal frames, the beam weight

slightly decreased for eccentricities up to around 72 in. (Figure 16). However, the parameter study showed that for eccentricities greater than 72 in. with single-diagonal frames, beam weight increases (Figure 16).

CONCLUSIONS

This paper discussed the formulation of design equations for BRBFs with eccentricity. The analysis methods for determining the shear, axial force, and bending moment demands for capacity design of beams and columns were presented. Then, nine BRBF designs representing two building heights (3 and 12 stories), two bracing configurations (chevron and single-diagonal), and various eccentricities were shown to demonstrate the impact of eccentricity on BRBF member sizing and weights.

The study supports the following conclusions:

- For BRBFs with chevron configuration, brace steel weights (steel cores, lugs, and outer casings) were similar regardless of eccentricity. The heavier brace cores for the chevron BRBF with eccentricity were offset by the reduced brace lengths.
- For BRBFs with a chevron configuration, the beam weight increases significantly with eccentricity, while the column weight increases more slowly. This slower increase in column weight is due to the offset effect of the beam-end shears, which increase with eccentricity but partially counteract the rise in vertical brace forces transmitted to the columns due to eccentricity.
- For chevron BRBFs, the 12-story design cases with eccentricities were 1.10 to 1.27 times heavier than the concentric case for eccentricities of 1 to 2 times the beam depth. The 3-story design case with eccentricity of 2 times the beam depth was 1.32 times heavier than the concentric frame. The difference in weight was almost entirely due to heavier beams in the chevron BRBF with eccentricity.
- For nonalternating, single-diagonal BRBFs with eccentricities, the columns with the stubs help resist the story shear, leading to decreasing story shear resisted by the braces. Thus, both the required brace sizes and brace length decreased for an eccentricity of 2 times the beam depth, resulting in lower brace weight.
- For nonalternating, single-diagonal BRBFs with eccentricities of 2 times the beam depth, the beam weight slightly decreased with the brace eccentricity, while the column weight slightly increased with the eccentricity. The total steel weights of single-diagonal cases with eccentricity of 2 times the beam depth were less than the concentric cases by about 3% to 5%.
- For nonalternating, single-diagonal BRBFs with eccentricities, designed by sizing the braces for the entire story shears (neglecting moment frame action), the total frame weights for cases with eccentricity of 2 times the beam depth were greater than the concentric cases by about 4% to 6%.

REFERENCES

AISC (1990), *Seismic Provisions for Structural Steel Buildings,* American Institute of Steel Construction, Chicago, Ill.

AISC (2016a), *Seismic Provisions for Structural Steel Buildings*, ANSI/AISC 341-16, American Institute of Steel Construction Chicago, Ill.

AISC (2016b), *Specification for Structural Steel Buildings*, ANSI/AISC 360-16, American Institute of Steel Construction, Chicago, Ill.

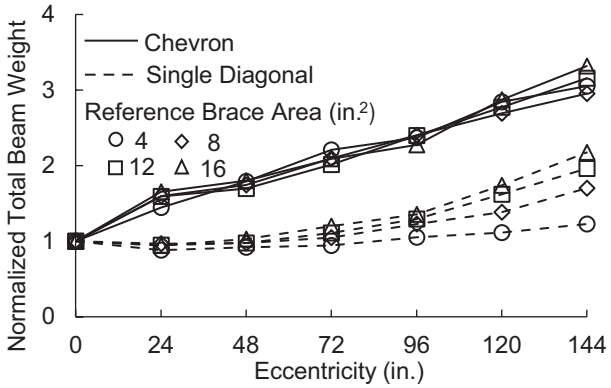

Fig. 16. Normalized beam weights for various eccentricities when beam depth is increased to use the most efficient shapes.

AISC (2022a), *Seismic Provisions for Structural Steel Buildings*, ANSI/AISC 341-22, American Institute of Steel Construction, Chicago, Ill.

AISC (2022b), *Specification for Structural Steel Buildings*, ANSI/AISC 360-22, American Institute of Steel Construction, Chicago, Ill.

ASCE (1993), *Minimum Design Loads for Buildings and Other Structures*, ASCE 7-93, American Society of Civil Engineers, New York, N.Y.

ASCE (2016), *Minimum Design Loads and Associated Criteria for Buildings Structures*, ASCE/SEI-7-16, American Society of Civil Engineers, Reston, Va.

ASCE (2022), *Minimum Design Loads and Associated Criteria for Buildings and Other Structures*, ASCE/SEI-7-22, American Society of Civil Engineers, Reston, Va.

ASTM (2022), *Standard Specification for Structural Steel Shapes*, ASTM A992/A992M, ASTM International, West Conshohocken, Pa.

CSI (2019), *CSI Analysis Reference Manual for SAP2000, ETABS, SAFE and CSiBridge*, Computers & Structures, Inc., Berkeley, Calif.

Engelhardt, M.D. and Popov, E.P. (1992), "Experimental Performance of Long Links in Eccentrically Braced Frames," *Journal of Structural Engineering*, Vol. 118, No. 11, pp. 3,067–3,088.

Fortney, P.J. and Thornton, W.A. (2017), "The Chevron Effect and the Analysis of Chevron Beams—A Paradigm Shift," *Engineering Journal*, Vol. 54, No. 4, pp. 263–296.

Hines, E. and Jacob, C. (2010), "Eccentric Braced Frame System Performance," Structures Congress, Orlando, Fla.

Hjelmstad, K.D. and Popov, E.P. (1983), "Cyclic Behavior and Design of Link Beams," *Journal of Structural Engineering*, Vol. 109, No. 10, pp. 2,387–2,403.

Hosseini, S.M. and Amiri, G.G. (2017), "Successive Collapse Potential of Eccentric Braced Frames in Comparison with Buckling-Restrained Braces in Eccentric Configurations," *International Journal of Steel Structures*, Vol. 17, No. 2, pp. 481–489.

Kasai, K. and Popov, E.P. (1986), "Cyclic Web Buckling Control for Shear Link Beams," *Journal of Structural Engineering*, Vol. 112, No. 3, pp. 505–523.

Lejano, B.A. and Mas, M.J.S. (2017), "Numerical Study on the Effect of Structural Parameters on the Behavior of BRBF-E," The Third International Conference on Civil Engineering Research (ICCER), Surabaya, Indonesia.

Li, C.-H., Richards, P.W., and Saxey, B.W. (2026), "Seismic Design and Performance of Buckling Restrained Brace Frames with Eccentric Brace Configurations Part 2: Analysis Studies and Design Implications," *Engineering Journal*, AISC, Vol. 63, No. 1, pp. 75–108.

Malley, J.O. and Popov, E.P. (1984), "Shear Links in Eccentrically Braced Frames," *Journal of Structural Engineering*, Vol. 110, No. 9, pp. 2,275–2,295.

NIST (2010), *Evaluation of the FEMA P-695 Methodology for Quantification of Building Seismic Performance Factors* (GCR 10–917–8), National Institute of Standards and Technology, Gaithersburgh, Md.

Prinz, G.S. and Richards, P.W. (2012), "Seismic Performance of Buckling-Restrained Braced Frames with Eccentric Configurations," *Journal of Structural Engineering*, Vol. 138, No. 3, pp. 345–353.

Roeder, C.W. and Popov, E.P. (1978), "Eccentrically Braced Steel Frames for Earthquakes," *Journal of Structural Engineering*, Vol. 104, No. 3, pp. 391–412.

Sabelli, R. and Arber, L. (2017), "Design of Chevron Gusset Plates," S*EAOC Convention Proceedings*, San Diego, Calif.

Shakib, H. and Safi, R. (2012), "Behavior Evaluation of the Eccentric Buckling-Restrained Braced Frame under the Near-Fault Ground Motions," 15th World Conference on Earthquake Engineering, Lisbon, Portugal.

Timoshenko, S.P. and Gere, J.M. (1961), *Theory of Elastic Stability,* 2nd Ed., McGraw-Hill Book Company, New York, N.Y.

Vayda, P.T. (2015), *Comparative Analysis of Buckling-Restrained Braced Frames in Eccentric Configurations (BRBF-Es) and Eccentrically Braced Frames (EBFs),* University of Arkansas, Fayetteville, Ark.